Development of Aluminium Injection Moulding Binder for Automotive Parts

TANAPAT WONGWATTANAKORNCHAI

A THESIS SUBMITTED IN PARTIAL FULFILLMENT

OF THE REQUIREMENT FOR THE DEGREE OF

MASTER OF ENGINEERING IN AUTOMOTIVE ENGINEERING

(INTERNATIONAL PROGRAM)

INTERNATIONAL COLLEGE

KING MONGKUT'S INSTITUTE OF TECHNOLOGY LADKRABANG

2013

KMITL-2013-IC-M-004-023

Thesis Title	Development of Aluminium Injection Moulding Binder for Automotive Parts
Student	Mr. Tanapat Wongwattanakornchai
Student ID.	51061903
Degree	Master of Engineering
Program	Automotive Engineering (International Program)
Year	2009
Thesis Advisor	Dr. Panya Kansuwan Dr. Anchalee Manonukul Assoc. Prof. Dr. Kunio Takahashi

ABSTRACT

This work studied the development of metallurgy powder (PM) technique which adapted to used for the aluminium metal injection moulding (Al MIM). The starting material was Al-Si-Cu-Mg alloy powder. This work was divided into two parts which were focused on the sinterability of compaction and sintering aluminium alloy affected by the sintering conditions and the injection moulding of Al-Si alloy. In the first part, the Al-Si alloy powder was compacted into the tensile test specimens with the average density of 2.5 g/cm^3. Those green specimens were sintered under six sintering conditions, in which the varied purity of nitrogen was 99.5% (industrial grade), 99.99%, and 99.999% atmosphere. In additional, the another factor was the present of sacrificial magnesium (Mg) weather Mg chips was added surround the specimens. The Mg chips act as an oxygen and moisture getter. The dewaxing and sintering temperature profile was 420°C for 1 hour and 560°C for 1 hour. It was found that sintering by using the flow controlled 99.5% purity of nitrogen and without sacrificial Mg produced the suitable sintered properties. The results from higher purity of nitrogen did not show significant improvement of the sintered properties. Sample sintered with sacrificial Mg shown poorer sintered properties with the present of aluminium nitride (AlN) observed by X-ray diffraction (XRD). The second part was to studied the Al MIM process by applying the different binder systems which are self-mixed and commercial binder (MRM). The green specimens were sintered by using the suitable sintering obtain from the experiment in the first part. It was found that the commercial binder (MRM) was more applicable than self-mixed binder. The commercial binder was using solvent

debinded (Hexane) and thermal debinded at 400°C for 2 hours. However, there was still some difficulty to achieve successful sintering.

ACKNOWLEDGEMENT

This thesis could not be completed without the assistance of many persons to whom I would like to express my sincere appreciation.

First, I would like to sincerely thank my advisor, Dr. Anchalee Manonukul, who has given me many helpful suggestions, useful advice and fruitful discussions during the undertaken research. I would also like to sincerely thank Dr. Panya Kansuwan, Dr. Wuttipong Rungseesantivanon for kind advising and helping, and Assoc. Prof. Dr. Kunio Takahashi for the suggestion.

Moreover, I would like to acknowledge ECKA Granulate, GmbH, Germany, for supplying the aluminium alloy powder. I would like to show gratitude to National Metal and Materials Technology Center (MTEC), especially the Metal Injection Moulding (MIM) laboratory for providing the laboratory equipments and instruments as well as financial supporting.

I am grateful to National Science and Technology Development Agency (NSTDA), which provided the full scholarship for studying in the master program.

Special thanks go to MTEC MIM laboratory's members for helping me during the experiment.

Finally, I am very grateful to my family for all love, caring, understanding and motivation throughout my life.

Tanapat Wongwattanakornchai

CONTENTS

CONTENTS (CONT.)

Page

CONTENTS (CONT.)

Page

CONTENTS (CONT.)

LIST OF TABLES

LIST OF FIGURES

Figure Page

LIST OF FIGURES (CONT.)

LIST OF FIGURES (CONT.)

CHAPTER 1

INTRODUCTION

1.1 Significance and Background

The growing demand for more fuel-efficient vehicle to reduce energy consumption and air pollution is the challenge for the automotive industry. Aluminium and its alloys become a competitive choice and used in several automotive parts, including sliding and frictional parts. Aluminium-silicon alloys (Al-Si alloy) have been of particular interest as this material offers the advantages of high-wear resistance, good temperature resistance and low coefficient of thermal expansion (Vukcevic and Delijic, 2002). The traditional process to manufacture aluminium alloy powders are pressed and sintered into the high-tolerance components. On the other hand, powder metallurgy (PM) has a limitation for produce parts with a smaller section thickness and complex shape.

Metal Injection moulding (MIM) is a manufacturing method combining the traditional PM process and plastic injection moulding. MIM process is ideally suited for the production of small and complex parts in large quantities and requires little or no secondary operation. Hence, it is extremely attractive for hard metals, high precision and high performance parts. The components commercially fabricated through MIM are commonly made of ferrous metals. However, there are some non-ferrous metal that can be commercially processed by MIM, such as titanium or nickel and their alloys.

The key issue in the development of MIM for alumnium is the sinterability. Poor sinterability of aluminium causes low sintered density and hence poor physical and mechanical properties. There are some studies to improve sinterability such as, the sintering aluminium alloy in different atmospheres, i.e. nitrogen, argon, nitrogen/hydrogen, and nitrogen/argon (Pieczonka, 2007). It was found that nitrogen was the most suitable controlled atmosphere. However, there is no previous study about the purity of the nitrogen gases and the present of sacrificial magnesium. In addition, there have been limited number of researches focusing on the aluminium injection moulding (Al-MIM) process for example vacuum processing (Tan and Ma, 2004) and sintering aid with tin or magnesium (Liu *et al.*, 2008; Liu *et al.*, 2009). However, these process are kept on the tread secret.

Most of previous works were conducted for the commercial PM process but there still limited understanding. In addition, Al-MIM using vacuum processing is very expensive and not practical. Therefore, this work studied can divide into two parts. The first part is the study of Al-Si alloy sinterability by varying the purity of nitrogen gas and sintering with or without sacrificial magnesium. It was the significant parameter in the sintering process of aluminium, but its effects in the sinterability was not clear in previous works (Pieczonka, 2007; Liu, 2008) and there was no system metric study about this parameter. The second part studied the fabrication of Al-Si alloy using common MIM process. The formulation of binder blends were compared between the self-mixed and commercial binder. Then, the debinding parameters were studied. Debinding profiles were designed for the different binder compositions. Finally, the suitable sintering profile from the study in the first part was adapt to the sinter the samples. Although this work concentrated in gaining more understanding of aluminium sintering and Al MIM fabrication process, this is a good step towards the MIM of aluminium.

The originality of this work was to study the effect of purity of nitrogen gas and effect of sacrificial magnesium to produce the small and complex parts by using aluminium injection moulding process with the commercial process. Firstly, the study was carried out in the sintering of aluminium. Sintering atmospheres, that were commonly used in aluminium sintering process, include nitrogen, argon, vacuum and the mixture of nitrogen and hydrogen gases (Schaffer *et al.*, 2006). Among these four atmospheres, it has been found that nitrogen is the most effective but, there has no previous study about the purity of nitrogen effect. Hence, the variation of nitrogen purity from 99.5 - 99.999% were examined in this work. The present of sacrificial magnesium effect has not previous corrected the data systematically (Liu *et al.*, 2008). Hence, the present of sacrificial magnesium were also sintered for all different purity of nitrogen gas. The suitable sintering condition from the first part was applied to the aluminium injection moulding parts. The focus of this work was to use common metal injection moulding equipment for aluminium injection moulding. The further work which can produce mass production of small and complex aluminium parts with cheaper process price

1.2 Objectives

1.2.1 To study the effects of sintering conditions by varying the purity of nitrogen gases and the present of sacrificial magnesium.

1.2.2 To study the difference between self-mixed and commercial binder on the MIM of aluminium alloy.

1.3 Scopes

1.3.1 The first part was on the compaction and sintering process of aluminium alloy powder by using the sintering aid technique.

1.3.2 Several purity of nitrogen gases and the present of sacrificial magnesium during sintering were studied.

1.3.3 The second part was on the fabrication of Al-Si-Cu-Mg alloy using commercial metal injection moulding (MIM).

1.3.4 The self-mixed and commercial binder were studied the sinterability of Al MIM binder.

1.3.5 The suitable sintering condition from the first part was selected to applied to used as the sintering condition.

1.3.6 The physical and mechanical properties were studied such as density, shrinkage, percentage of binder loss, X-ray diffraction (XRD), macroscopic hardness, and tensile properties.

1.4 Expected Benefits

1.4.1 Understanding the processing method for aluminium parts through the powder metallurgical process.

1.4.2 Understanding the metal injection moulding processing for aluminium parts.

1.4.3 Understanding the process mechanism occurred during debinding.

1.4.4 Being able to use the basic scientific equipments and characterisation instruments for material science and engineering study.

1.4.5 Useful research works which can be extended to the actual applications in the automotive industries or more advanced applications.

CHAPTER 2

LITERATURE REVIEWS

2.1 Introduction of Aluminium Powder Metallurgy (Al-PM)

Aluminium alloys and composites are attractive for the automotive and aerospace industry, which is seeking cost-effective weight reduction. This leads to reduction in the fuel consumption for their products (Hunt, 1998). In addition, aluminium alloy offer advantages of high wear resistance, high strength, good electrical and thermal conductivity (Heard *et al.*, 2009). Additionally, there is significant industrial potential for aluminium alloys fabricated by net-shape powder metallurgy (PM) techniques including lower production cost and high reliability of products(Nishiyabu *et al.*, 2004; German and Bose, 1997).

PM is a near-net-shape manufacturing process in which metallic powders are pressed and sintered into the nearly finished or finished parts. Die compaction or pressing process is also known as the conventional PM process which is the most commonly parts forming. The basic steps consists of compaction of powder into a shape, and applying heat or sintering in a controlled atmosphere and a temperature below the melting point of the major constituent. The conventional PM process can be economically produced parts such as, gear, connecting rod, camshaft, and pulley and oil gear pump.

Another form of PM process, which becomes an interesting trend for production of small and complex parts, is metal injection moulding (MIM) process. The MIM process combines a small quantity of polymeric binder with metal powders to form feedstock that can be injection moulded. This process uses the shaping advantage of injection moulding process. After moulding, the next process is used to extracted the binder, which is called debinding. Some of binder was still remained to hold the skeleton of metallic powder. Finally, the sintering similar to the conventional PM process was applied to complete the process of MIM (Cheremisinoff, 1998). The major difference between the conventional PM and MIM process is the forming step. In the conventional PM process, the specimen is formed in the compacted solid using high pressure. On the other hand, in MIM the

specimens is shaped in semi-solid form by less pressure. Hence, it is possible to inject parts with higher shape complexity and smaller than conventional PM (German and Bose, 1997). Another different point is debinding process, MIM process needs the debinding process before moving to sintering process, while the conventional PM process can combined the debinding directing to the sintering process. **Figure 2.1** show the main process of metal injection moulding

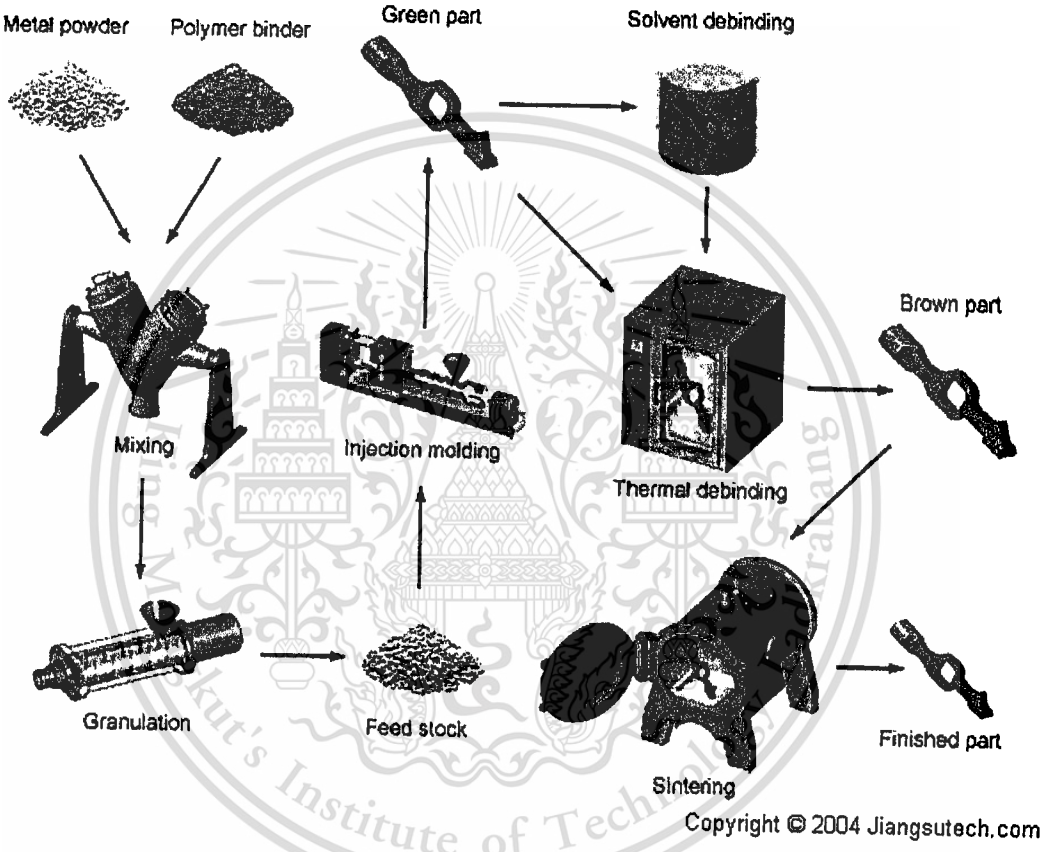

Figure 2.1 Metal injection moulding process (http://www.prlog.org/11733325-metal-injection-molding-mim-parts.html)

The aluminium sintering is on-going research and still under developing stage because sintering of aluminium is difficult. This is due to the oxide layers that effect the sinterability of aluminium. The oxide layer is always present and covered the powder surface. Therefore, these layers is need to be removed or disrupted in order to enable and enhance sinterability of aluminium.

In addition, the MIM process has great potential and numerous advantages. However, much of the process technology has been kept in commercial secret. One of the major technical challenges is the formulation for suitable binder system for optimizing the moulding and debinding characteristic of the MIM process.

2.2 The Parameter in Sintering of Aluminium PM Processing

2.2.1 The Effect of Sintering Aids

Although magnesium is a common reducing agent during sintering of aluminium, there is still the limitation of magnesium addition. It was found that the maximum content less than 1% by weight of magnesium could reduce the oxide through the formation of spinel ($MgAl_2O_4$), but this was dependent on the aluminium particle size as shown in **Figure 2.2** (Lumley *et al.*, 1999). It shows that more magnesium was required to sinter smaller powders because of the greater surface area and hence more amount of oxide. Furthermore, the addition of more than 1% by weight caused the net expansion of specimens as shown in **Figure 2.3**. This is due to the excess magnesium diffused into the base metal, especially from the liquid phase (Fuentes *et al.*, 2003; Lumley *et al.*, 1999).

Copper (Cu) is one of the primary alloying elements for aluminium and can be used as sintering aid. The major influence of copper is on the tensile properties of sintered aluminium (Schaffer, 2004). Sintering of aluminium with copper always occurred in transient liquid phase sintering (Schaffer *et al.*, 2001), in which total Cu in the liquid solution is drawn into the aluminium and when Cu is completely dissolved, the liquid solution is disappeared. However, the major problem in sintering of aluminium-copper alloy system is the diffusivity of copper in aluminium is 5000 times greater than that of aluminium in copper and hence causes the expansion of the sintered specimen. Therefore, sintering of the Al-Cu system should be carefully controlled and is dependent on the process variables.

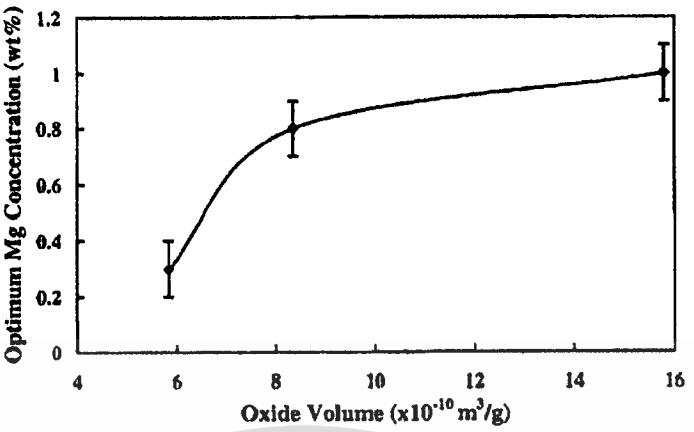

Figure 2.2 The concentration of magnesium required to achieve maximum densification in binary aluminium-magnesium alloy as a function of oxide volume (Lumley *et al.*, 1999).

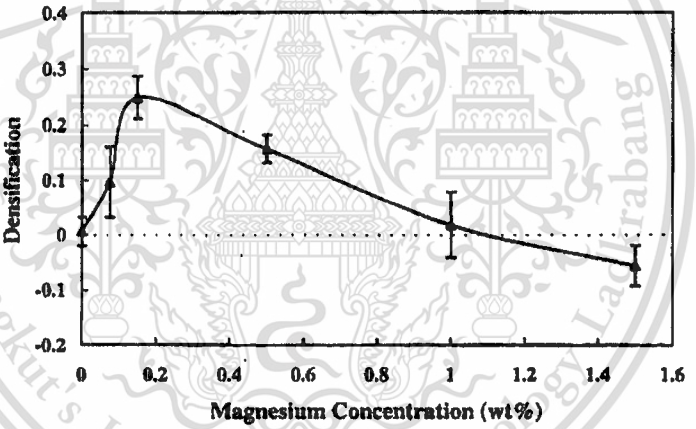

Figure 2.3 The effect of magnesium on the densification of aluminium powder. The densification[1] was maximised at 0.15% wt. of Mg, and there was net expansion at concentrations more than 1% by weight (Lumley *et al.*, 1999).

[1] Densification is a parameter that indicates the ability to densify of the sintered compact relative pore free compact from its green stage (German, 1996). Densification value is given by $\psi = \frac{\rho_s - \rho_g}{\rho_t - \rho_g}$, where ρ_s is the sintered density, ρ_g the green density, and ρ_t the theoretical density. The positive value indicates there is shrinkage occurred while negative value indicates expansion.

Silicon (Si) is another possible sintering aid that always presented as a major alloying element in the 6xxx series alloy, and a minor addition in the 2xxx series alloy. In 6xxx series alloy, silicon enhances the sinterability through the formation the liquid phase with aluminium and magnesium (Showaiter and Youseffi, 2007; Youseffi *et al.*, 2006). In the 2xxx series alloy, the volume of liquid phase is slightly increased by adding silicon in small amount causing the improvement of tensile strength (Schaffer, 2004). However, pressureless sintering of pure aluminium with high content of silicon was found to be unfeasible to obtain high sintered density. Alternative process, such as hot pressing was applied to achieve high density (Yilmaz and Altintas, 1996).

The main concept of this method is based on the reduction mechanism by adding another element that is more reactive to oxygen than aluminium into an aluminium powder system. It was found that the addition of magnesium (Mg) in the aluminium powder system could reduce the aluminium oxide to reveal the underlying aluminium atoms and facilitate sintering (Lumely *et al.*, 1999; Fuentes *et al.*, 2003)

Magnesium can reduce the oxide of aluminium resulting formation of two species, $MgAl_2O_4$ (Spinel) and magnesium oxide (MgO). The forming reaction of these two species are shown as followed (Kimura *et al.*, 2001; McLeod and Gabryel, 1992):

$$3Mg + 4Al_2O_3 \rightarrow 3MgAl_2O_4 + 2Al \quad (2.1)$$

$$3Mg + Al_2O_3 \rightarrow 3MgO + 2Al \quad (2.2)$$

However, these formations depend on the magnesium content and temperature, which they are formed as observed by Xie *et al.* (2005). In aluminium rich magnesium alloy, MgO is dominantly occurred, while $MgAl_2O_4$ is dominantly occurred in aluminium lean magnesium alloy at the experimental temperature. However, at the critical content of magnesium, there is a change between MgO to $MgAl_2O_4$ with an increasing experimental temperature (Xie *et al.*, 2005).

Lumley *et al.* (1999) concluded about the reduction mechanism of aluminium oxide by the addition of magnesium and represented the reduction mechanism as shown in **Figure 2.4**. It shows that at the Mg-oxide contact site, local MgO can occur due to the relative rich of magnesium.

Magnesium diffuses along the metal-oxide interface and through the aluminium powder and then reduces the oxide at the metal-oxide interface. Nearby aluminium particles, which are not directly in contact with magnesium powder, are subsequently exposed to the reductance and their oxide layers are disrupted.

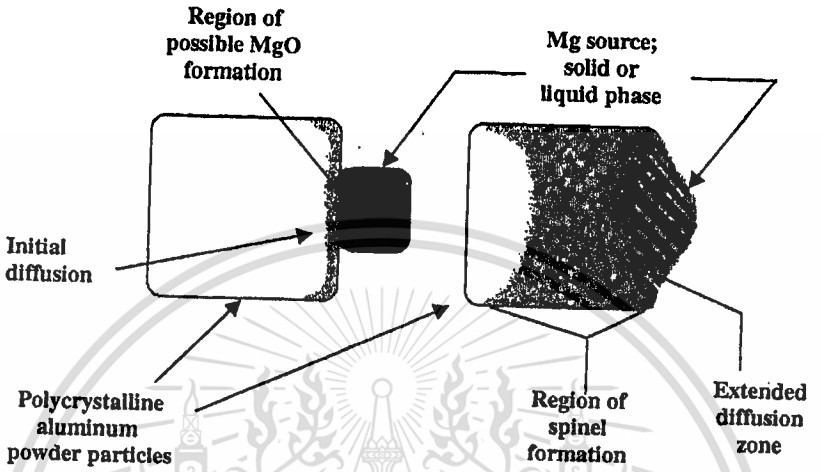

Figure 2.4 A schematic representation of the processes involved in the reduction of the alumina layer by magnesium during the sintering of Al-Mg alloys (Lumley *et al.*, 1999).

In addition, for the pre-alloyed powder of aluminium containing magnesium as an alloying element, the dissolved magnesium in the powder particles migrates into the surface oxide and is saturated in the composition where the Mg/Al ratio is about 0.5 during heating. When the sintering temperature is reached, magnesium reduces aluminium oxide at the particle surfaces, resulting in the breakage of the surface oxide layers and eventually appearance of metallic aluminium on the outer surface of the powder particles (Kimura *et al.*, 2001). **Figure 2.5 (a)** shows the TEM observation at the region of bonding interface between two particles of aluminium alloy containing 0.3% wt. of magnesium. The corresponding high magnification image in **Figure 2.5 (b)** was taken from the square frame as shown in **Figure 2.5 (a). Figure 2.5 (b)** shows the Al-Mg grain at left and right-hand side and a lot of precipitates observed at the interface. Therefore, further analysis by EDS was taken at these specific areas, designated as *A*, *B*, and *C* in **Figure 2.5 (b).** The results are found that at the area *A*, the peaks of oxygen, aluminium and magnesium were observed, which were more

likely to be $MgAl_2O_4$. While the areas *B* and *C* were observed to be Al-Mg matrix and pure Al respectively (Xie *et al.*, 2005).

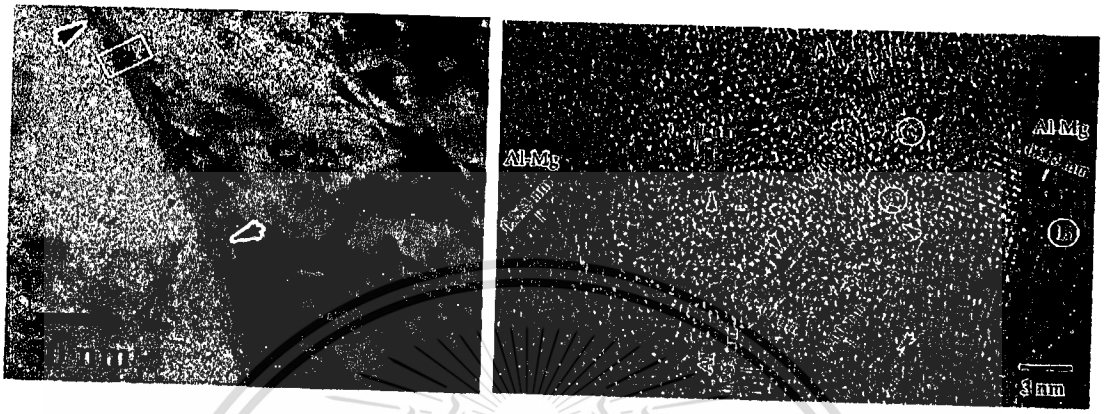

(a) (b)

Figure 2.5 TEM micrographs of Al–0.3Mg alloy specimen, (a) a bright-field TEM image, (b) corresponding high magnification TEM image taken from the square frame in (a), which is the interface region of bonding (Xie *et al.*, 2005).

Apart from magnesium that plays an important role in the reduction mechanism, there are other sintering aids that can be added into an aluminium system in which based on the common alloying elements that always presented with aluminium, namely copper (Cu), zinc (Zn), and silicon (Si). These elements play a role in formation of liquid phase during sintering (Schaffer *et al.*, 2001). Sercombe (1998) stated about the role of liquid phase forming during sintering that the eutectic liquid could penetrate the oxide layers at the crack caused by compaction. The melt could then diffuse through the cracks, lifted the oxide layers and allowed metal-metal bonding to occur. Moreover, when the additive phase became solid solubility in aluminium, expansion caused by diffusion of these elements into solution may cause oxide fracture.

Although sintering with the presence of sintering aids seems to have expansion of the specimen by the diffusion of those additives into aluminium matrix, shrinkage during sintering is also occurred by the mechanism of liquid phase sintering itself (German, 1996; Schaffer *et al.*, 2008).

MacAskill *et al.*, (2010) compared the effects of magnesium and nitrogen on the sintering response. The magnesium addition can improved the sintering response of the aluminium powder and increased the propensity for reaction with gaseous nitrogen. Aluminium nitride (AlN) was confirmed as the principal reaction product. On the other hand, tin was ineffective as a sintering aid for pure aluminium powder when present as the sole alloying addition.

SEM images of the sintered microstructures observed in pure aluminium and Al–1.5Mg alloys are shown in **Figure 2.6**. The poor sinter quality in the compact of aluminum powder was clear given the abundance of prior particle boundaries, minimal interparticle necking, and the lack of pore rounding. The sinter quality was improved with the addition of magnesium regardless of the source employed. Hence, prior particle boundaries were less discernible and an appreciable level of pore rounding was evident.

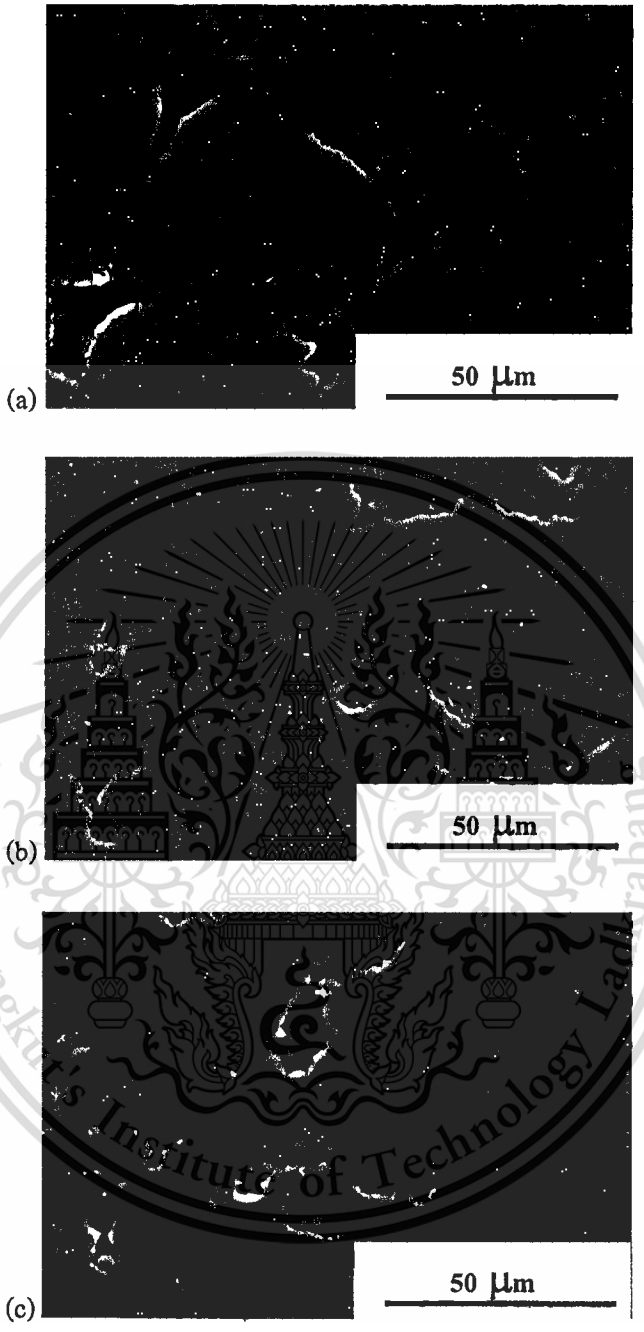

Figure 2.6 SEM images of (a) pure Al, (b) Al–1.5Mg sintering aids and (c) Al–1.5Mg master alloy type (MacAskill *et al.*, 2010)

2.2.2 The Effects of Compaction Pressure

Applying high compaction pressure can disrupt the oxide layers through the plastic deformation of aluminium powder resulting in cracks occurred at the point where the powders touch each another. This can be explained by the compaction phenomenon (German, 1994) that the powder initially has the density approximately equal to the apparent density after die filling. Applying initial pressure causes rearrangement of the powders to fill the large pore giving a higher packing density. Increasing pressure provides better packing and leads to decrease porosity with the formation of new particle contacts. The contact points then undergo elastic deformation. Higher pressures increase the density by contact enlargement through plastic deformation. However, increasing higher pressure, the density is not increased significantly due to the entire powders become work hardened. Therefore, the change in density as a function of compaction pressure can be illustrated in Figure 2.4.

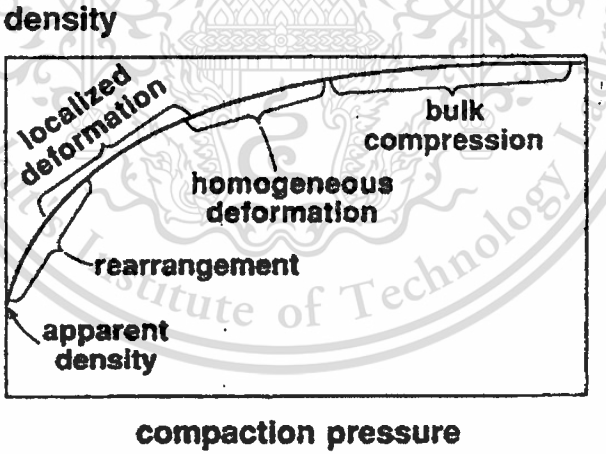

Figure 2.7 A sketch of the density versus compaction pressure during compaction of metal powder, showing key stages and declining compressibility as the density increases (German, 1994).

Gutin *et al.* (1972) investigated the effects of compaction pressure on the sintered properties, i.e. strength and relative electrical conductivity, of both lightly and severely oxidized

aluminium powders compact. For the oxidised aluminium powder, **Figure 2.8 (a)** shows that with increasing compaction pressure, the strength of the sintered specimens increased, while their electrical conductivity gradually increased and nearly approached that of the bulk aluminium specimen. In the case of oxidized aluminium powder, as shown in **Figure 2.8 (b),** the trend of the result is similar to that of **Figure 2.8 (a)** but there was less variation of both strength and relative electrical conductivity obtained from sintered specimens comparing with their green specimens. However, this shows the evidence that the applying high compaction pressure was more effective for the lightly oxidized powders because the oxide films were disintegrated into small fragment, enabling large contact area to be formed. For the severely oxidized powders, applying high compaction pressure was not as effective, but the additional application of the sheer force helped to intensify film rupture, enabling some contact area appeared (Andreeva and Rastrigina, 1965).

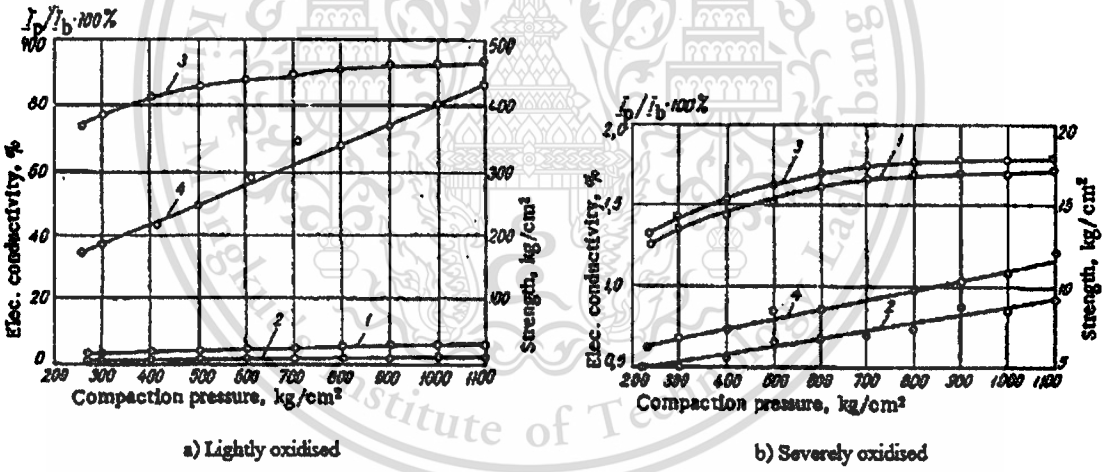

Figure 2.8 Effects of compaction pressures on the strength and relative electrical conductivity of both green and sintered specimens of (a) lightly oxidised and (b) severely oxidised aluminium powder, whereas 1 and 3 represent the green and sintered electrical conductivities and 2 and 4 represent the green and sintered strength respectively (Gutin *et al.*, 1972).

Heard *et al.*, (2009) showed that Al-15Si-2.5Cu-0.5Mg (Alumix 231) green strength increased with increasing compaction pressure as shown in **Figure 2.9**. This occurred due to the

increasing extent of mechanical inter-locking between the soft aluminium and the hard master alloy powder particles.

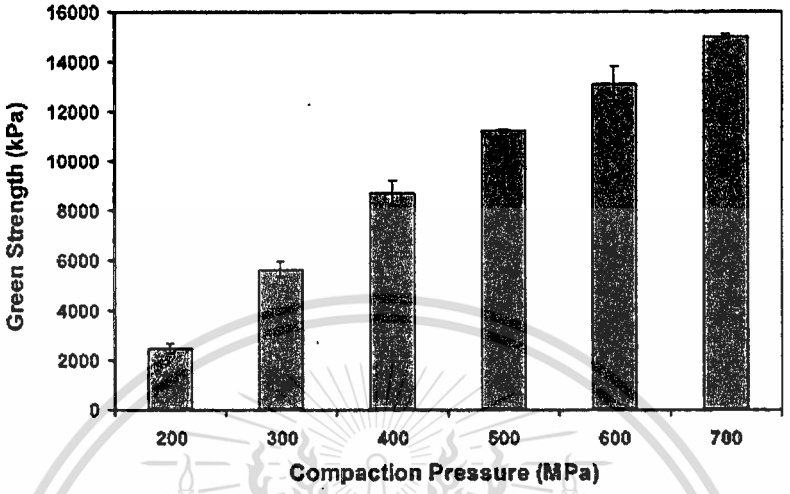

Figure2.9 Green strength as a function of compaction pressure for Alumix-231 (Heard *et al.*, 2009).

2.2.3 The Effects of Sintering Atmosphere

The sintering of pure aluminium powder was carried out in different sintering atmospheres, i.e. nitrogen, argon, nitrogen/hydrogen and nitrogen/argon gas mixtures, and also in vacuum. Pure nitrogen was found to be the only active sintering atmosphere for aluminium, promoting shrinkage associated with a weight gain by binding nitrogen, and enhancing mechanical properties of the sintered compacts. Hydrogen lowers the sinterability of aluminium very strongly, even when presents in small concentrations in a nitrogen atmosphere. Electron spectroscopy was used to characterise the surface layers on aluminium powder particles, fractured green compacts and sintered samples. Distributions of aluminium, nitrogen, oxygen and other elements, contained as impurities, were obtained by depth profiling measurements on this surfaces.

Sintering atmosphere is an important factor that plays a significant role during sintering, especially for aluminium, because it must act as an oxidising protector and/or partial reducing agent. Sintering atmospheres, that commonly used in aluminium sintering process, include nitrogen, argon, vacuum and mixture of nitrogen and hydrogen gases (Schaffer *et al.*, 2006). Among these four atmospheres, it has been found that nitrogen is the most effective (Pieczonka *et al.*, 2007;

Schaffer and Hall, 2002; Schaffer *et al.*, 2006). **Figure 2.10** shows the effects of sintering atmosphere on the densification of Al-3.8Cu-1Mg-0.7Si. The zero minute corresponds to the time at which the sintering temperature was first attained. Samples expanded initially under all atmospheres and then shrink over time, except where hydrogen was added to the gas stream, when no shrinkage occurred. With the other three atmospheres, the shrinkage rate was the same for the first 10 minutes, but it slowed down thereafter in argon and accelerated under nitrogen. Therefore, it showed that the efficiency of the sintering atmosphere decreased in the order: nitrogen > vacuum > argon > the mixture of nitrogen and hydrogen gases (Schaffer *et al.*, 2006). Nitrogen is effective for not only aluminium alloy but also pure aluminium as investigated by Pieczonka *et al.* (2007).

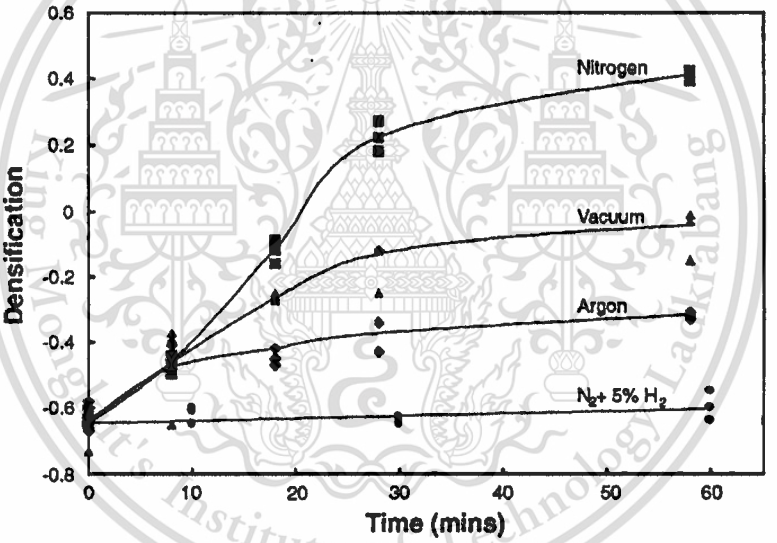

Figure 2.10 The densification of Al–3.8Cu–1Mg–0.7Si as a function of time and atmosphere (Schaffer *et al.*, 2006).

Nitrogen is not only the protective atmosphere during sintering but also acts as the reducing agent, while the others act as only the protective atmosphere. It is suggested that there is the formation of aluminium nitride (AlN) occurred when aluminium is sintered in nitrogen (Schaffer and Hall, 2002; Schaffer *et al.*, 2006). This formation comes from two reactions; the first comes from the partial reduction of Al_2O_3 by the reaction:

$$2Al_2O_3 + 2N_2 \rightarrow 4AlN + 3O_2 \quad (2.3)$$

and/or the second is the direct reaction with nitrogen according to:

$$2Al + N_2 \rightarrow 2AlN \quad (2.4)$$

In addition to the sintering atmosphere, another oxidising agent during sintering of aluminium is the water vapour or moisture. The relevant parameter of the water vapour is known as dew point. The dew point is the temperature at which the water vapour will condense and it is used to indicate the level of water vapour content in the atmosphere (Lutgens and Tarbuck, 1998). Ideally, the required atmosphere dew point in order to completely reduce aluminium oxide is -140°C at sintering temperature of 600°C (Lumley *et al.*, 1999), which is difficult to reach. In practice, a dew point of -40°C is rather arbitrarily defined as the maximum allowable water level (Dudas and Dean, 1969). Higher level of moisture is detrimental to the properties as shown in **Figure 2.11**. The sintering response of Al-3.8Cu-1Mg-0.7Si is retarded at dew point more than -60°C. However, for dew point higher than -60°C, the powder compact showed less densification and was begun to expand (Scahffer *et al.*, 2006). This is suggested that the water vapour acts as the stabiliser of aluminium oxide, which hinders shrinkage due to one of the stable phases of aluminium oxide is the hydrated aluminium oxide (Krajnikov *et al.*, 2002; Scahffer *et al.*, 2006).

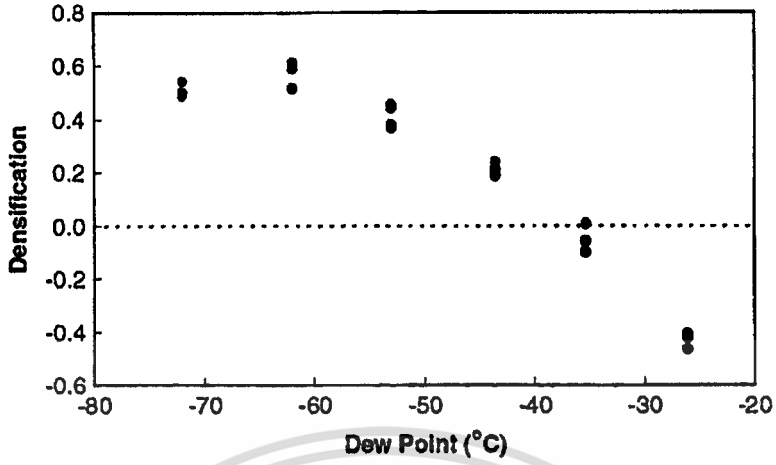

Figure 2.11 Effect of dew point of nitrogen on the densification of Al–3.8Cu–1Mg–0.7Si, pressed at 100 MPa and sintered for 30 minutes (Schaffer *et al.*, 2006).

2.2.4 The Effects of Sacrificial Magnesium

Liu *et al.*, (2008) used magnesium block as the sacrificial material when the aluminium alloy 6061 with tin was sintered in nitrogen atmosphere condition. Without these magnesium pieces, the outer surface does not sinter and the outer few millimeters can be scrapped off with a fingernail. There is no reported regarding the mechanical and physical properties when the specimens were sintered with or without magnesium block.

2.2.5 The Effect of Aging Hardening

The apparent hardness of the sample alumix 231 was shown in **Figure 2.12** as a function of sintering temperature and time (1 hour, 1 week) after sintering, with respect to the sintering temperature. This increase was associated with a post-sinter natural age-hardening response commonly observed in aluminum PM alloys (Heard *et al.*, 2009; Kent *et al.*, 2005).

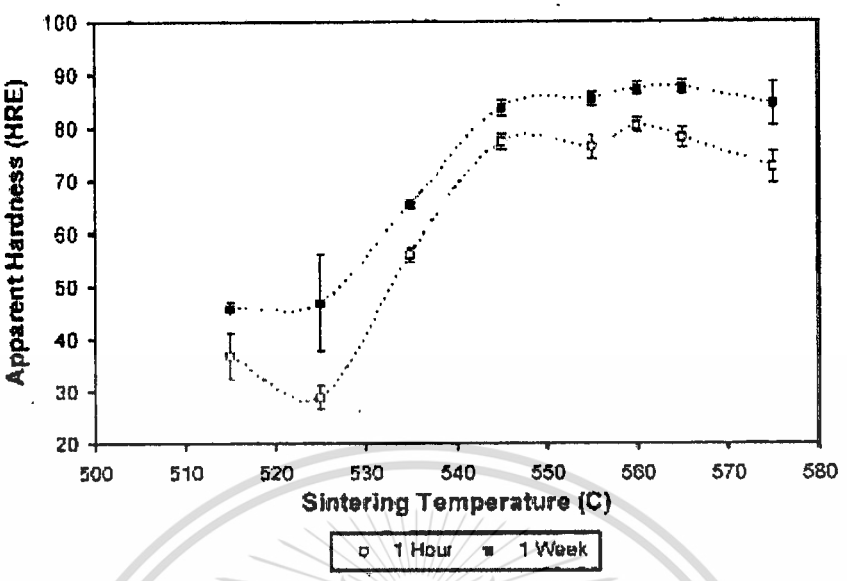

Figure 2.12 Apparent hardness of Alumix-231 as a function of sintering temperature and time (1 h, 1 week) after sintering (Heard *et al.*, 2009).

2.3 The Parameters of Aluminium Metal Injection Moulding (Al-MIM)

The steps involved in forming a component by metal injection moulding (MIM) include the following: (1) selecting and tailoring a powder for the process; (2) mixing the powder with a suitable binder; (3) producing homogeneous granular pellets of mixed powder and binder; (4) forming of the part by injection moulding in a closed die; (5) processing the formed part to remove the binder (debinding); (6) dandifying the compact by high-temperature sintering; and (7) post-sintering processing as appropriate (German and Bose, 1997)

2.3.1 The Sintering Aid Effect on Al-MIM

The AlN was pre-mixed before the mixing with binder to investigate the effect of AlN in aluminium injection moulding (Liu *et al.*, 2009). The poor sintering on the surface still appeared as shown in **Figure. 2.13.**

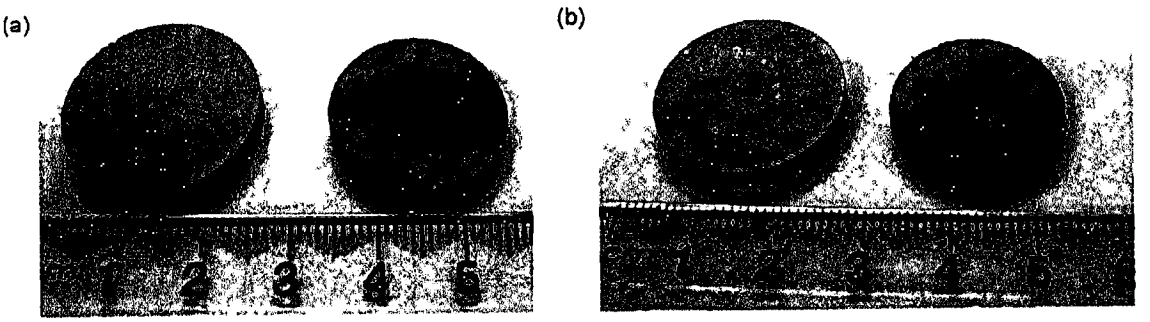

Figure 2.13 Green and sintered surfaces of (a) the top surface (AA6061 + 2Sn) and (b) the bottom surface (AA6061 + 2Sn + 10AlN). The sintered parts are distortion free (Liu *et al.*,2009)

Tin (Sn), which is another possible sintering aid to the aluminium (AA6061) powder were mixed. Tin is generally a beneficial additive for the enhanced liquid phase sintering of aluminium. The effect of tin makes a sintering response of AA6061 produced higher density than without tin addition (Liu *et al.*, 2008)

2.3.2 Binder Formulation

The binder formulation is the key component in MIM. It controls the mixing. moulding and debinding operations. It also strongly influences the maximum powder loading in the feedstock, the green strength of the moulded parts, and the shape retention of the parts during debinding (Foong and Tam, 1998; German and Bose, 1997). Therefore the binder formulation in aluminium metal injection moulding is still under developed, some binder formulation and processing detail are kept as the trade secret (Tan and Ma, 2004; Liu *et al.*, 2009; Liu *et al.*, 2008).

2.3.3 Mixing processing

The aluminium powder was mixed with binder and sintering under the vacuum atmosphere which is cannot produce with the conventional MIM process (Tan and Ma, 2004) and the cost of vacuum process is higher than usual. In addition, another variable from the mixing conditions such as powder loading, temperature and mixing speed could affect to the shrinkage during debinding and sintering (Supati *et al.*, 2000). The feedstock properties also affect the moulding process by the viscosity decreases with increasing shear rate and temperature (Liu *et al.*, 2003)

2.3.4 Debinding

The binder must be removed from the moulded specimens prior to its densification by sintering, at the same time without causing any defect in green parts. Thermal debinding of a thermoplastic based binders are by far the most widely used. In addition, the solvent debinding was applied to reduced the time of thermal debinding. After solvent debinding, the compact is dried to remove the solvent from the pore. Subsequently, the remain polymer is extracted by burnout (Tsai and Chen, 1995; Germen and Bose, 1997; Liu *et al.*, 2008; Liu *et al.*, 2009)

CHAPTER 3

EXPERIMENTAL PROCEDURES

3.1 Experimental Procedures

3.1.1 Introduction

The overall experimental procedures in this work can be divided into two main parts shown as a flow chart in **Figure 3.1.** This work was based on the commercial aluminum alloy powder which supplied from ECKA Granulate, GmbH, Germany. The powder used in this study was the air-atomised aluminium-silicon-copper-magnesium (Al-Si-Cu-Mg) alloy. Its commercial name is Alumix 231. The product information shown in **Appendix A.**

There are two parts in this study. Part one is the study using compaction process and part two, is the study using MIM process. In part one, the powder was compacted into dog-bone tensile specimens, which is called "green"specimens by pressing machine. Then, the green specimens were debinded and sintered by using the profile was shown in **Figure 3.2.** In this part, two main parameters, that were studied, are the purity of nitrogen and the present of magnesium on the sinterability of sintered Al-Si alloy.

In part two, the fabrication of Al-Si alloy by using MIM was investigated. Al-Si alloy powder and polymer binders was mixed and formed an intermediate product called "feedstock". Subsequently, the feedstock was formed into a dog-bone tensile specimen by injection moulding. The product from this step was called "green"specimen. The green specimen was debinded by solvent and thermal debinding process. "Brown" specimens were obtained after the binder was removed from green specimens. Sintering was a final step of MIM. Sintering profile and condition were selected from the optimum sintering condition from Part 1 of the experiment.

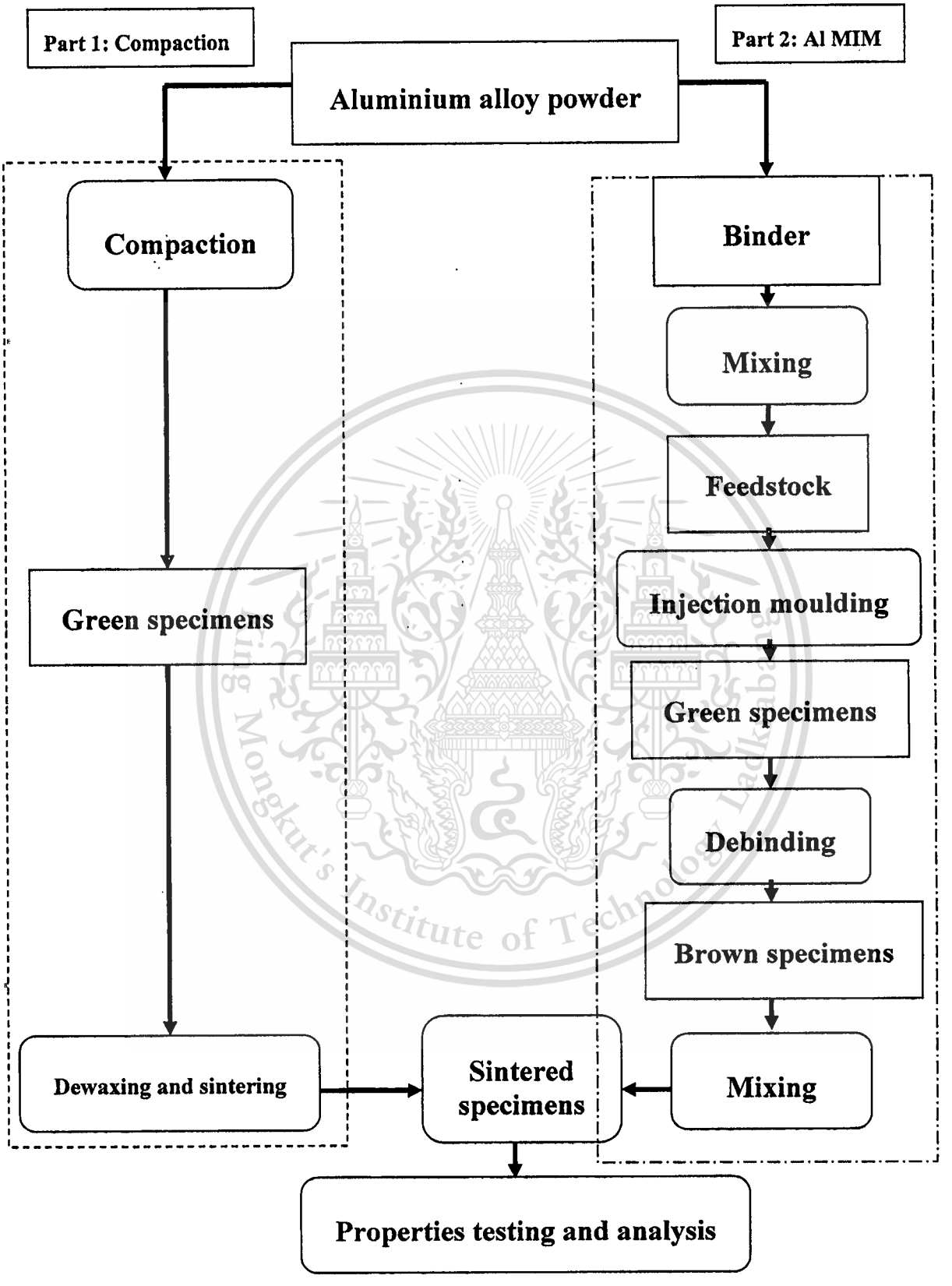

Figure 3.1 Flow chart of the commercial powder metallurgical (PM) process.

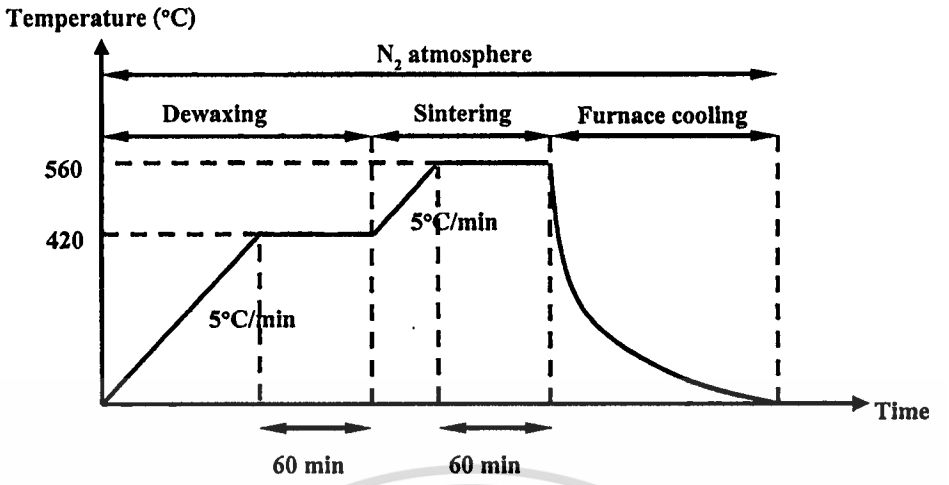

Figure 3.2 Thermal cycle for sintering (Salee *et al.*, 2009)

After sintering, sintered parts from both parts of the experiment were examined to determine the properties, microstructure and oxide content. The methodology to examine the properties of specimens of specimens will be explained in detail later.

3.1.2 The Effects of Purity of Nitrogen and the Present of Sacrificial Magnesium on Sinterability (Part 1)

The aluminium alloy powder used in this study for both parts of the experiment was admixed with the 1.5% by weight of Ethylene-bis-stearmide wax. The chemical compositions were Al-15Si-2.5Cu-0.5Mg (% by weight). The scanning electron image of this powder was shown in **Figure 3.3** (Salee *et al., 2009*). The powder were clustered together by the admixed wax as visible in the **Figure 3.3.** The aluminium alloy powder was initially compacted into tensile specimens with green density of 2.50±0.01 g/cm^3 using the compaction pressure of 700 MPa. For sintering conditions, there were six different sintered conditions as shown in **Table 3.1.** There are two main parameters, which are the purity of nitrogen and the present of sacrificial magnesium. The varied of purity of nitrogen were 99.5% (industry grade), 99.99%, and 99.999%. The magnesium (Mg) chip was produced by machining Mg block into smaller chip form and cleaned by alcohol. 6 grams for each sinter batch the sacrificial magnesium was placed in the crusibles next to the sintered. Samples was shown in **Figure 3.4.**

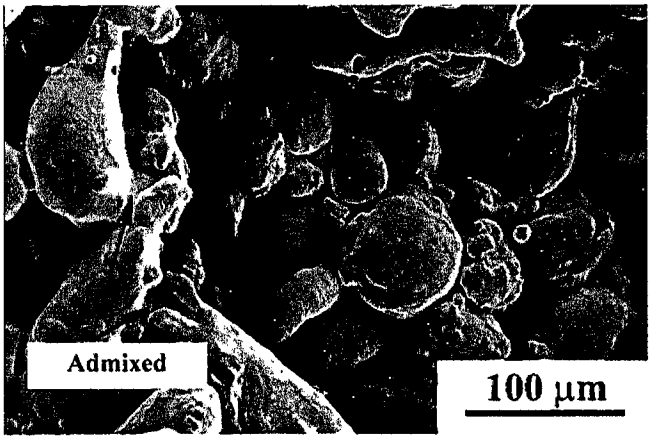

Figure 3.3 Scanning electron micrograph of the aluminium alloy used in this study. The powders clustered together by the admixed wax (Salee *et al.,2009*).

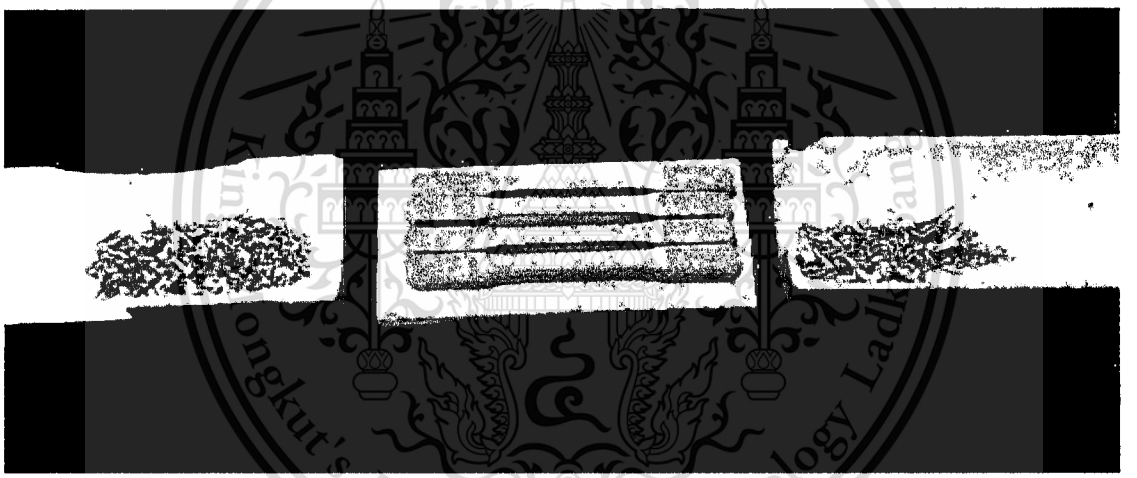

Figure 3.4 Sintering setup with the present of sacrificial magnesium.

Table 3.1 Variation of sintering conditions

Purity of nitrogen gas (%)	Sacrificial magnesium
99.5	Without
99.99	
99.999	
99.5	With
99.99	
99.999	

3.1.3 Fabrication of Al MIM (Part 2)

In this part, two different binders were used, which are self-mixed and commercial binders.

The self-mixed binder formulation contains with 3342M poly polypropylene (PP), paraffin wax (PW), and stearic acid (SA). All components were supplied from the local supplier. On the other hand, the commercial binder(MRM) was supplied by Mould Research Co.,Ltd, Japan. The commercial binder is polyacetal based binder (Kanakawa,1998).

3.1.3.1 Mixing Process

For the self-mixed binder, the powder and binder were mixed preliminary in a mixer. The binder system consisted of 70% by weight of paraffin wax, 25% by weight of polypropylene and 5% by weight of stearic acid. The pre-mixed powders and PP were first blended together. Subsequently, polypropylene was melted paraffin wax and stearic acid were added. The mixing time was hold for 30 minutes to ensure homogeneity. The dough-type mixture was removed from the chamber and cooled down to room temperature. The cold mixture was crashed into small pieces of feedstock ready for injection moulding. The powder loading was investigated and varied in this self-mixed binder.

For the commercial binder (MRM), the powder loading was 54.4% vol. The powder and binder were pre-mixed before added to the chamber. The mixing chamber was heated to 160°C. Then, the pre-mixed powder was added to the chamber until the binder was melted and the mixing was kept continuing at this temperature for another 30 minutes to ensure

homogeneity. The feedstock was removed from the heated chamber similar to the self-mixed process and crashed.

3.1.3.2 Moulding

Feedstock was moulded using hot pressing and injection moulding. Disc sample of 15 mm in diameter were prepared using hot compaction for the self-mixed binder. 1.8±.2 g feedstock was loaded into the mould. The mould temperature was varied from 80-100°C.

For the commercial binder, the feedstock was injected into be tensile specimens by a metal injection moulding machine. **Table 3.2** shows the successful condition that is used for injected the specimens.

Table 3.2 Injection moulding condition for commercial Binder (MRM)

Injection time (s)	Cooling time (s)	Injection speed (mm/s)	Injection pressure (MPa)	Nozzle temperature (°C)	Moulding temperature (°C)
5	15	30	80	175	45

3.1.3.3 Debinding and Sintering

In part two, the suitable sintering condition from the part one was used for sintered the specimens after debinded. Brown parts from debinding transferred to sinter at 560°C for 1 hour in nitrogen.

For debinding process of the self-mixed binder, green parts were thermally debinded in air. The heat rate was slow at 0.4°C/min from 40-400°C. In addition, the temperature was hold at 90, 230, 320 and 400°C for an hour. Specimens were furnace cooled to room temperature.

For debinding process of the MRM binder, the debinding condition is shown in **Table 3.3.** Eight conditions were used as shown in **Table 3.3**. The solvent debinding with hexane (industrial grade) was applied in some conditions to investigate the characteristic

with the same temperature at 40°C before transferred to a new setter and debinded with thermal debinding. Atmosphere of debinding can separated into two types, which are air and nitrogen atmospheres.

Table 3.3 Debinding conditions

Debinding condition	Solvent debinded holding time (Hours)	Thermal debinding temperature (°C)	Holding time (Hours)	Atmosphere	Type of furnace
1	Without	260	2	Air	Fine Furnace
2		340	2		
3		340	2	N_2	Tube Furnace
4		340	3		
5		450	2		
6		450	3		
7	4	400	2		
8	8	400	2		

3.2 Testing of Properties

3.2.1 Physical Properties

3.2.1.1 Density

The density measurement was based on the Archimedes' principle. This corresponds to the standard test method of ASTM B311 (ASTM International, 2005). The density can be calculated as follows:

$$\rho = \frac{(m_a \times \rho_w)}{(m_a - m_w)} \tag{3.1}$$

where, ρ = the density of test specimen (g/cm^3),

m_a = mass of test specimen in air (g),

m_w = mass of test specimen in water (g),

ρ_w = the density of water at the measuring temperature (g/cm^3).

The green density was not measured for all specimens to minimize the reaction of aluminium with water. Water submersion could cause the water to residual within the pores and then would deteriorate the sinterability of aluminium powders. Therefore, only the green density of one specimen from every five pieces was measured. It is possible to control the deviation of density to be ±0.01 g/cm^3. However, the sintered density was measured for all specimens (Salee *et al., 2009*).

3.2.1.2 Shrinkage measurement

The shrinkage of the sintered specimens was measured relative to their green specimens. The measurement was taken at five specific positions as shown in **Figure 3.5** and each position was designated as W_1, W_2, W_3, L, and T.

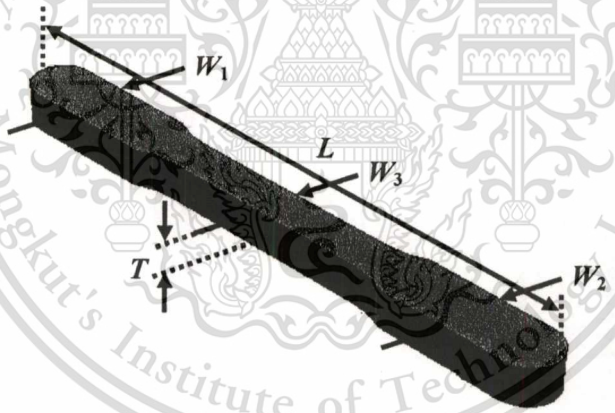

Figure 3.5 The specific positions for measuring dimension in the specimen.

The shrinkage of the sintered specimens from their green stage can be calculated as follows:

$$Shrinkage = \frac{(D_g - D_s)}{D_g} \times 100 \qquad (3.2)$$

where, Shrinkage = the shrinkage in which the positive sign indicates shrinkage, while the negative sign indicates expansion (%),

D_g = the dimension at a specific position of the green specimen (mm),

D_s = the dimension at a specific position of the sintered specimen (mm).

3.2.1.3 Relative Oxide Analysis

The effect of oxide have no previous measured the quantity of oxide on the specimens. Takahashi (2008) suggested a technique to determine the relative oxide contents by using the scanning electron microscope (SEM) equipped with the energy dispersive spectroscopy (EDS). By this technique, the unknown oxygen contents in the aluminium alloy specimen were measured relatively to the aluminium oxide or alumina (Al_2O_3). The calculation of the relative oxide content can be explained as follows:

Considering the electron beam with intensity, I, projected on alumina (Al_2O_3) specimen, the percentage by weight of aluminium detected by EDS, $W_{Al(Al_2O_3)}$ can be represented as a function of beam intensity as follows,

$$W_{Al(Al_2O_3)} = \frac{2}{5} k_{Al} I \tag{3.3}$$

where, $W_{Al(Al_2O_3)}$ = the percentage by weight of aluminium in Al_2O_3 detected by EDS (% wt.),

k_{Al} = the proportional constant for aluminium,

I = the intensity of electron beam,

and number $\frac{2}{5}$ is the ratio of 2 aluminium atoms from 5 atoms of Al and O in alumina (Al_2O_3).

The percentage by weight of oxygen detected by EDS, $W_{O(Al_2O_3)}$ can also be represented as a function of beam intensity in a similar way as follows,

$$W_{O(Al_2O_3)} = \frac{3}{5} k_O I \tag{3.4}$$

where, $W_{O(Al_2O_3)}$ = the percentage by weight of oxygen in Al_2O_3 detected by EDS (% wt.),

k_O = the proportional constant for oxygen,

and number $\frac{3}{5}$ is the ratio of 3 oxygen atoms from 5 atoms of Al and O in alumina (Al_2O_3).

Dividing Equation (3.4) by Equation (3.3) yields,

$$\frac{W_{O(Al_2O_3)}}{W_{Al(Al_2O_3)}} = \frac{3}{2}\frac{k_O}{k_{Al}} \tag{3.5}$$

The electron beam with the same intensity projected on the aluminium alloy specimen with unknown oxide content was considered. It is noted that the intensity should be equal if the same accelerating voltage is used. If x is the unknown value of oxygen content relative to aluminium content in an aluminium alloy sample, the ratio of oxygen to aluminium in the aluminium alloy specimen can be written as O : Al = x : 1. By using the same relation as Equations (3.3) and (3.4), the percentage by weight of aluminium, $W_{Al(Sample)}$, and oxygen, $W_{O(Sample)}$, detected by EDS can be represented as a function of beam intensity as follows,

$$W_{Al(Sample)} = \left(\frac{1}{1+x}\right)k_{Al}I \tag{3.6}$$

$$W_{O(Sample)} = \left(\frac{x}{1+x}\right)k_{O}I \tag{3.7}$$

where, $W_{Al(Sample)}$ = the percentage by weight of aluminium in aluminium alloy sample detected by EDS (% wt.),

$W_{O(Sample)}$ = the percentage by weight of oxygen in aluminium alloy sample detected by EDS (% wt.).

Dividing Equation (3.7) by Equation (3.6) yields,

$$\frac{W_{O(Sample)}}{W_{Al(Sample)}} = \frac{x}{1}\frac{k_O}{k_{Al}} \tag{3.8}$$

Substitution of $\frac{k_O}{k_{Al}}$ from Equation (3.5) into Equation (3.8) yields,

$$\frac{W_{O(Sample)}}{W_{Al(Sample)}} = \frac{x}{1}\cdot\frac{2}{3}\frac{W_{O(Al_2O_3)}}{W_{Al(Al_2O_3)}} \tag{3.9}$$

Therefore, the oxygen per aluminium contents value, X, can be calculated from the following equation,

$$x = \frac{3}{2}\cdot\frac{W_{Al(Al_2O_3)}}{W_{O(Al_2O_3)}}\cdot\frac{W_{O(Sample)}}{W_{Al(Sample)}} \tag{3.10}$$

From equation (3.10), it can be seen that if the measured sample is alumina (Al_2O_3), then X (the relative oxygen per aluminium content) will be 3/2.

3.2.1.4 Microstructure Preparation

The method to prepare specimens for microstructural observation started from the sintered specimen was cut into a small piece to reveal the cross section. The specimen was then hot mounted in the epoxy resin. To reveal the clear and smooth microstructure, the specimen was firstly ground by the silica papers and subsequently fine polished with the diamond suspension. The steps of the grinding and fine polishing (ASM International, 2004; Salee *et al.*,2009) were tabulated in **Table 3.4.**

Table 3.4 Grinding and fine polishing for aluminium PM specimens (ASM International, 2004)

Grinding					
Step	**Abrasive**	**Grade**	**Lubricant**	**Rotating speed (rpm)**	**Time (minute)**
1	SiC	500	H_2O	200	1-5
2	SiC	1000	H_2O	200	1
3	SiC	2400	H_2O	200	2.5

Fine polishing						
Step	**Cloth**	**Abrasive**	**Gradation**	**Lubricant**	**Rotating speed (rpm)**	**Time (minute)**
1	Nap	D.P.*	3 μm	Alcohol based	150	1**
2	Nap	D.P.*	1 μm	Alcohol based	150	1.5***

Note: * D.P. = diamond paste.

** If there were still scratches remaining from grinding step, the 1st step of fine polishing should be continued.

*** If there were still scratches appeared on the specimen, the 2nd step of fine polishing should be continued until the scratches were eliminated.

3.2.1.5 X-ray Diffractometer (XRD) Analysis

X-ray diffractometer (JEOL, JDX-3530, 2kW) was used to investigate the chemical reaction on the specimen. The measuring angle was measured from 10-90 degree. The raw and processed material such as Al-Si powder, MRM binder, and magnesium were measured. The results was shown the XRD results pattern could be read and match the chemical components by material data program Jade 5.0 (MacAskill *et al.*, 2010; Heard *et al.,* 2009).

3.2.1.6 Differential Scanning Calorimetry (DSC) Analysis

To determine the mixing temperature, the DSC analysis was used to fine the peak temperature, which shows the melting point of binder. The range and mixing temperature can be designed by using DSC results. The atmosphere conditions applied in these DSC analyses, which are Oxygen (O_2) and Nitrogen (N_2).

3.2.1.7 Thermogravimetric Analysis (TGA)

The studied mechanisms of thermal debinding of MIM parts can be observed by TGA curves. In this experiment, the TGA results in 2 different atmospheres were carried out for the MRM binders which O_2 and Nitrogen N_2. However, a self-mixed binder TGA result was measured under the O_2 only (German and Bose, 1997).

3.2.2 Mechanical Properties

3.2.2.1 Macro Hardness

The Rockwell scale F or HRF hardness test was selected to measure the apparent macroscopic hardness of the specimen. The specimen was kept for 1 week, which is the suitable time period for natural age hardening. The increase in hardness was associated with a post-sinter natural age hardening response commonly observed in aluminium PM alloy by Heard *et al.* (2009). The test was carried out by indenting the 1/16" steel ball with the applied load of 60 kgf for 6 seconds according to the standard test method MPIF standard number 43 (Metal Powder Industries Federation, 2002).

3.2.2.2 Tensile Properties

The other 4 pieces of sintered specimens were selected to test their tensile properties including ultimate tensile strength and elongation according to the standard test

method for determination of tensile properties of the P/M materials, MPIF standard number 10 (Metal Powder Industries Federation, 2002).

CHAPTER 4

THE EFFECT OF THE PURITY OF NITROGEN AND THE PRESENT OF SACRIFICIAL MAGNESIUM ON THE SINTERABILITY OF SINTERED ALUMINIUM ALLOY (Al-Si-Cu-Mg)

4.1 Effects of Sintering Conditions on Physical Properties

4.1.1 Density

The effect of sintering in different purity of nitrogen and with or without sacrificial magnesium (Mg) on density is shown in **Figure 4.1**. The sintered densities of sintered specimens in condition without sacrificial Mg with purity of nitrogen gases 99.5%, 99.99%, and 99.999% were 2.64, 2.65, and 2.64 g/cm^3 respectively. While, the sintered density of 2.61, 2.57, and 2.57 g/cm^3 were obtained for specimens sintered in 99.5%, 99.99%, and 99.999% with sacrificial Mg respectively. The result with different purity of nitrogen gas had no significant effect in the sintered density when the samples were sintered without the sacrificial Mg. However, when sintered with Mg samples sintered using 99.5% purity of nitrogen gas has density more than those sintered using higher purity of gas. For all purity of nitrogen sintered with Mg resulted in lower density than sintered without Mg. The results were repeated more than 10 times 4 piece of specimens measured. The results shown the same results as the **Figure 4.1.** Compared with Heard *et* al., (2007) and Arribas *et* al., (2010) was using the nitrogen for sintering atmosphere but different purity and have not any experiments studied the effect of varied the purity of nitrogen before. From Heard *et* al., (2007) show that the sintering temperature has more effect to the properties than the purity of nitrogen. However, the sintered density was decrease in condition sintering with sacrificial Mg. For sacrificial Mg was presented in Liu *et al.*, (2008) shown that the condition without sacrificial Mg block, the outer few millimeters can be

scrapped off with fingernail but have no result of physical or mechanical properties. In addition, this study used the different type of aluminium alloy from Liu *et al.*, (2008).

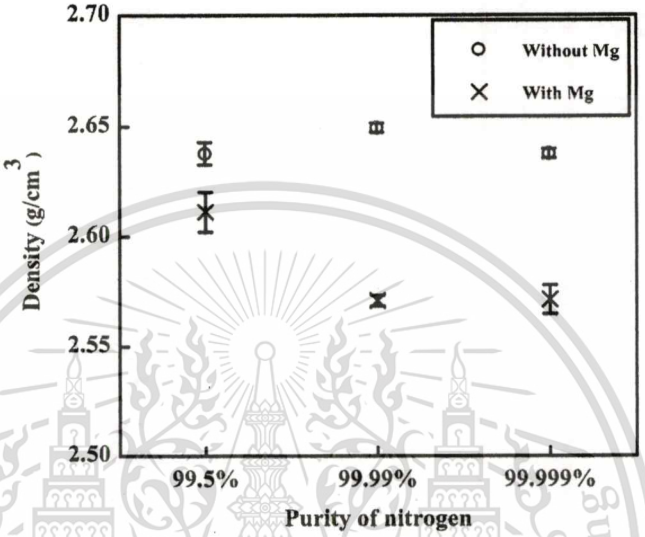

Figure 4.1 Density of the specimens sintered in different conditions.

Therefore, the moister content in the nitrogen gas has less significant increasing of density was observed the sintered density increased linearly for the purity of nitrogen. Z.Y. Liu *et al.* (2008) the effect from sacrificial gave opposite results, which meant that the key of sintered would composed with sacrificial Mg. In this study, different composite of alloy was used, this gives the opposite results of properties of sintered specimens. Detail will be discussed in more detail later.

4.1.2 Shrinkage Results

Figure 4.2. The result showed that the purity of nitrogen has an effect to the shrinkage but very little. The higher of gas purity give the higher shrinkage at every position and the shrinkage was decreased for condition with sacrificial Mg. This is in good agreement with the sintered density shown in **Figure 4.1.** The results of average width (W_{avg}) and length (L) were shown in the **Figure 4.2 (b)** and **4.2(c)** This show more deviation than the result in the thickness T. This could explain by the L side has a longer length for measure compare by ratio to the W_{avg} and T which has shorter

distance so, in term of measurement the specimens should be measured with care.

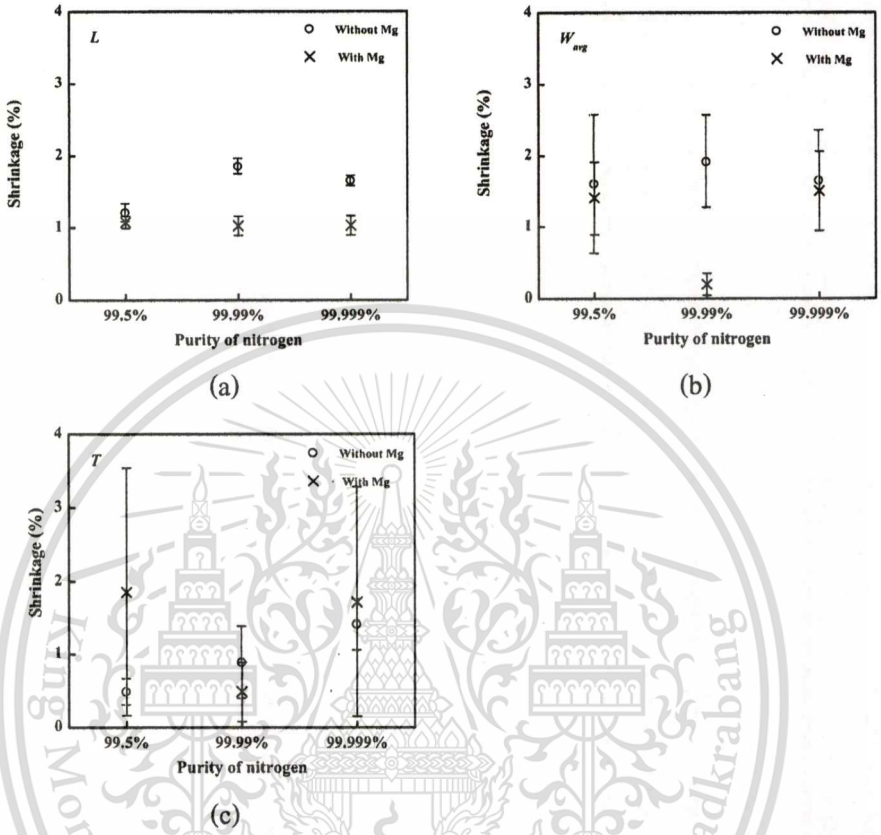

Figure 4.2 The linear shrinkage of the specimens at specific dimensions for different sintering condition (a) average width, (b) lenght (L), and (c) thickness (T) for each sintering condition (a) W_{avg}, (b) L, and (c) T.

The explanation of deviation (error bar) was studied with the results that shown in **Figure 4.3**. The specimens sintered with 99.5% purity of nitrogen without sacrificial magnesium were selected to explained the results. The specimen on setter position and the direction of gas flow was shown in Figure 4.3. The results show that the measurement with W and T side have less effect from the sintered position while, the L side show an opposite results.

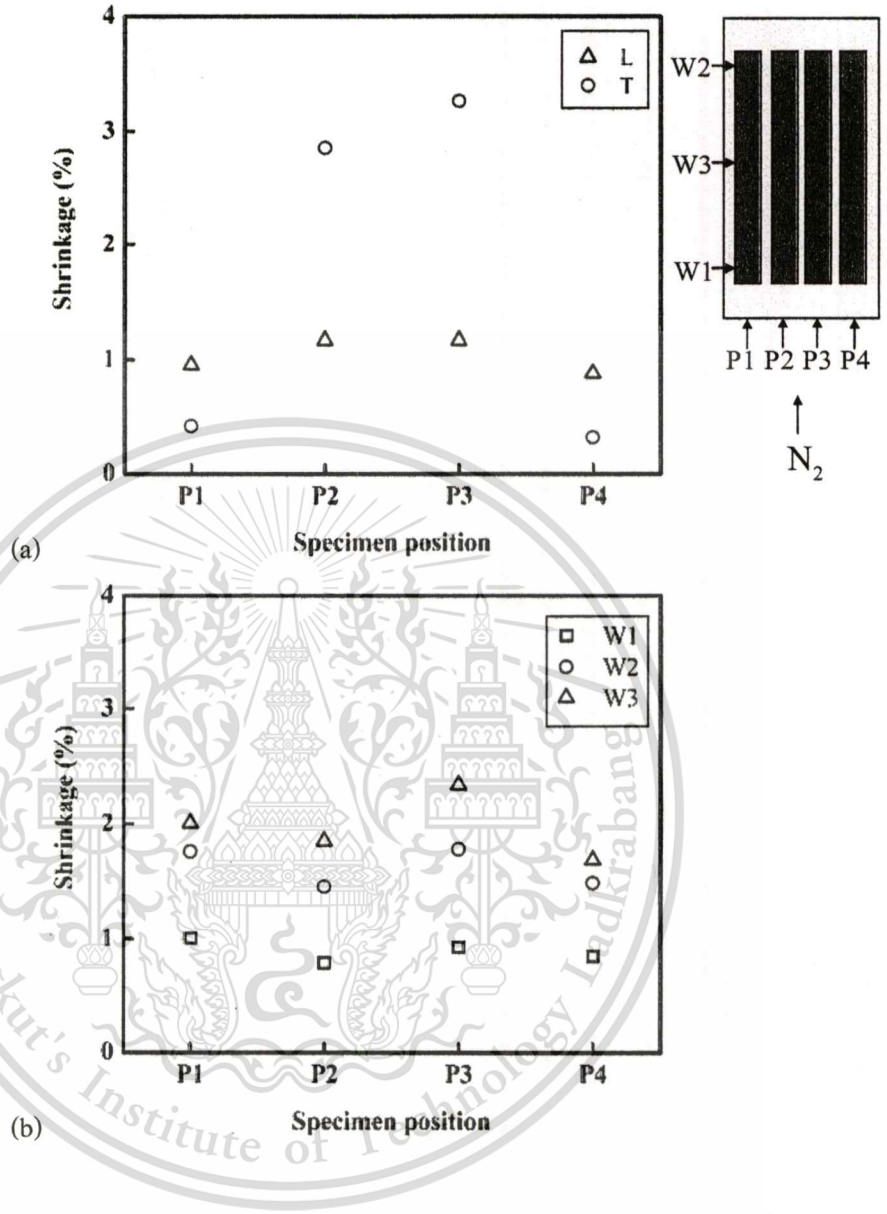

Figure 4.3 Linear shrinkage in specific dimension (a) length (L) and thickness (T) and (b) average width (W_{avg}) at different position in a tube furnace sintered with 99.5% purity of nitrogen gas.

The L measurements show that the position on the setter has an effect to the shrinkage rate. The specimens in P2 and P3 positions at the centre of the furnace show the higher shrinkage than the P1 and P4 position near by the wall of furnace. The effect of this deviation came from the slightly different temperature distribution in the tube furnace which at the centre of the furnace has higher

temperature than the specimens near by the wall of furnace. All of this explanation referred to the standard deviation of T have more wide range of error bar than W and L respectively.

4.1.3 Microstructure

The results shown from the previous section such as density and shrinkage have good agreement and show that the purity of nitrogen has very less effect to the sinterabiliy. The further investigate was concerning only with the 99.5% purity of nitrogen, which has a cheapest price from the selection purity of nitrogen. Then, the condition with and without sacrificial Mg could be observed.

Figure 4.4 shows the appearance of specimens sintered under the 99.5% purity of nitrogen without and with sacrificial Mg. Note that the appearance of specimens under different purity show similar trand, hence it is omitted here. With Mg, darker and also more pores can be observed using bare eyes. This supports that the sacrificial Mg did not enhance densification.

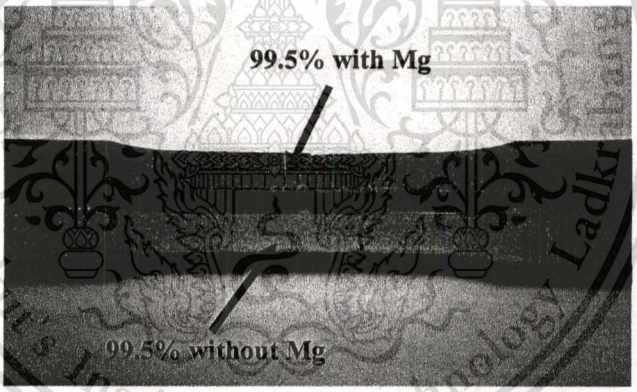

Figure 4.4 Photograph of sintered with and without sacrificial Mg by using 99.5% purity of nitrogen

The sinterability of Al-Si-Cu-Mg alloy was affected by the sintering conditions by the condition sintered with sacrificial magnesium shown the poor sinterability. **Figures 4.5 (a)** and **(c)** were the micrograph of the sintered without sacrificial Mg with 99.5% and 99.999% purity of nitrogen. Specimens in **Figures 4.5 (b)** and **(d)** show micrographs of the sintered specimens with sacrificial Mg under 99.5% and 99.999% purity of nitrogen. Moreover, the microstructure observation shows that, the specimen sintered in condition without sacrificial magnesium had the

most homogeneous dispersion of silicon phase with minimal porosity as shown in **Figures 4.5 (a)** and **(c)**. It is noted that the superficial of appearance specimen surface exhibited the similar microstructure to the centre, which consisted of pore distributed throughout the specimens. The key feature in the beneficial use of nitrogen is the formation of aluminium nitride (AlN) (Schaffer *et al.,* 2006), which referred to the pore filling mechanism after AlN was formed. On the other hand, the sacrificial magnesium used as the oxygen getter to improved the outer surface, but in this study Al-Si-Cu-Mg alloy give an opposite results. This showed that the presence of sacrificial magnesium could not improved the properties of sintered samples.

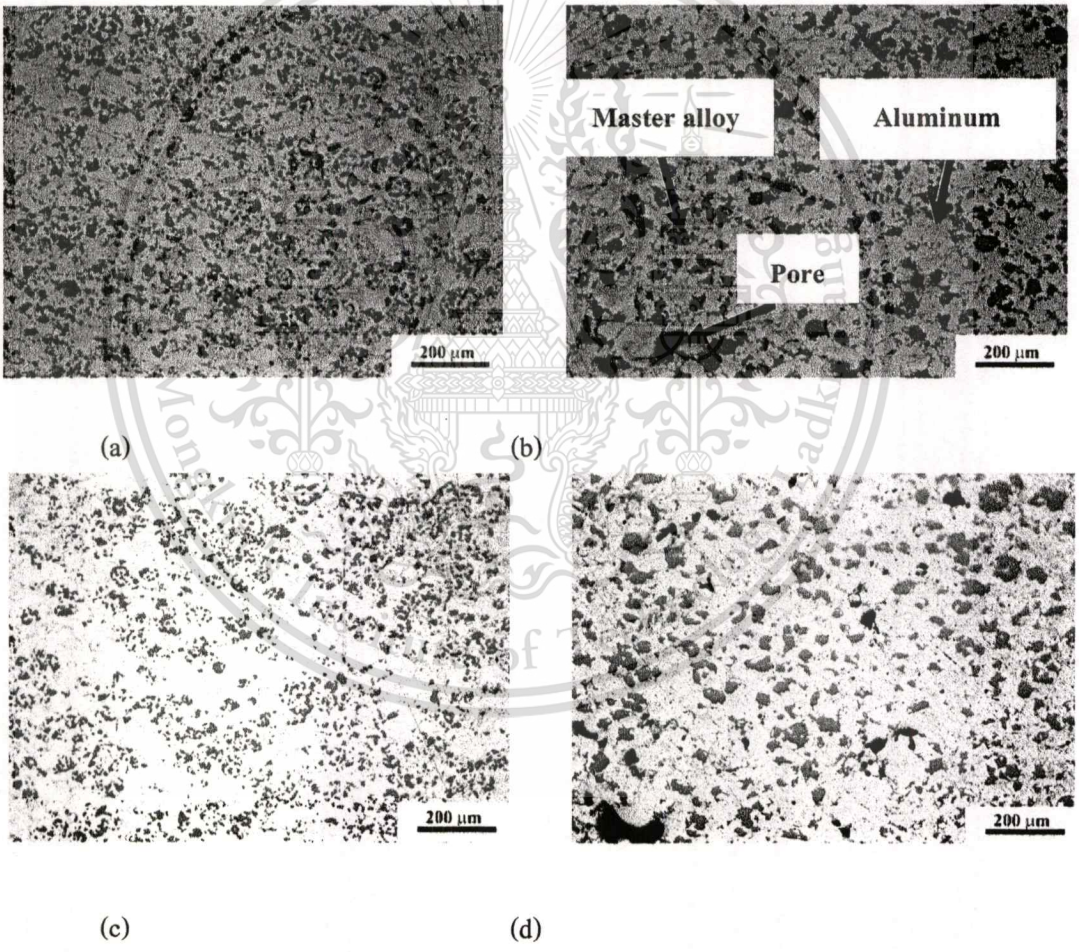

Figure 4.5 Microstructure from sintered with 99.5% purity of nitrogen was selected to compared between (a) without, and (b) with sacrificial Mg conditions. The conditions 99.999% (c) without and (d) with sacrificial Mg conditions

4.1.4 XRD results

The formation of AlN by the reaction of Al-Si alloy and nitrogen were identified by phases presented is XRD results in **Figures 4.6 (a)** and **(b)**. The resulting diffraction pattern recorded from the sintered specimen in condition without and with sacrificial magnesium by used 99.5% purity of nitrogen. On the specimens Al-Si alloys were the dominant phase but the presence of AlN was also verified. This confirms that the formation of AlN had appeared in this alloys and that this was the principal mechanism behind the observed mass gain. If compared the difference between **Figures 4.6 (a)** and **(b)**, the higher intensity of the graphs in sintering without sacrificial magnesium the phase of AlN was showed. This result showed that sacrificial Mg has disturbed the intensity results. From the study, the formation of AlN can improved the densification and sinterability by G.B. Schaffer *et al.* (2006), which has directly affected to the sinterability of Al-Si-Cu-Mg alloy microstructure by the formation of AlN.

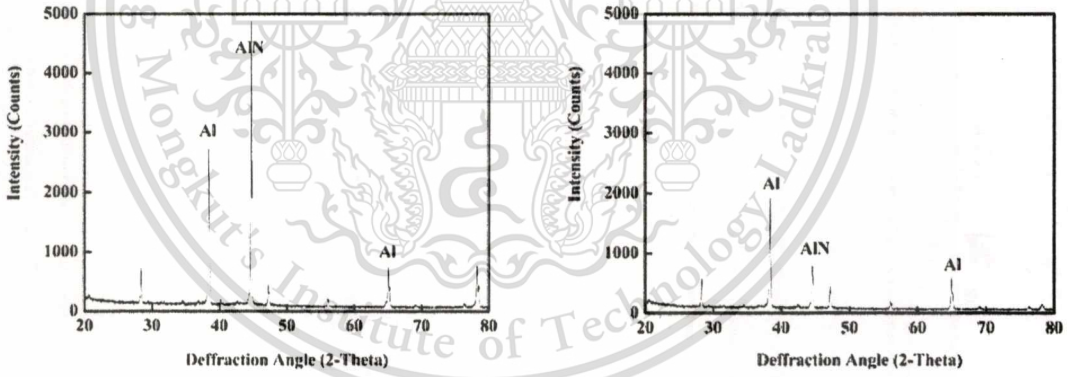

(a) (b)

Figure 4.6 An XRD pattern from the same purity of nitrogen (99.5%) but different conditions without (a) and with sacrificial (b) magnesium.

The formation of AlN was interrupted by used the sacrificial magnesium condition, which **Figure 4.7** was observed more detail of magnesium scraps between before and after used as the sacrificial materials. Initially, Mg sacrificial is produced by from machining Mg block into smaller chip form, then cleaning by alcohol and wait until dried. The reason to make Mg into a chip form is to increase the specific surface area and hence make it a better oxygen getter. Mg chip was added around sample without contact with sample. The Mg chip quantity used in this experiments is about 6 g. After sintering, sacrificial magnesium become brittle and flake. In addition, a number of white powder was observe around Mg chips as shown in **Figure 4.6 (a)**. **Figure 4.6 (b)** shown the corresponding XRD results of pure Mg chips before used and **Figure 4.6 (c)** shown the results after used as sacrificial material. XRD results shown the pure Mg element before use then, iron (Fe) from unknown where was found by the used Mg chip and also magnesium oxide. And white powder shown brucite $Mg(OH)_2$ which is resulted from using Mg for used as getter of oxide. This result shown that used the sacrificial magnesium has interrupted the AlN reaction or the contaminated the sintering atmosphere.

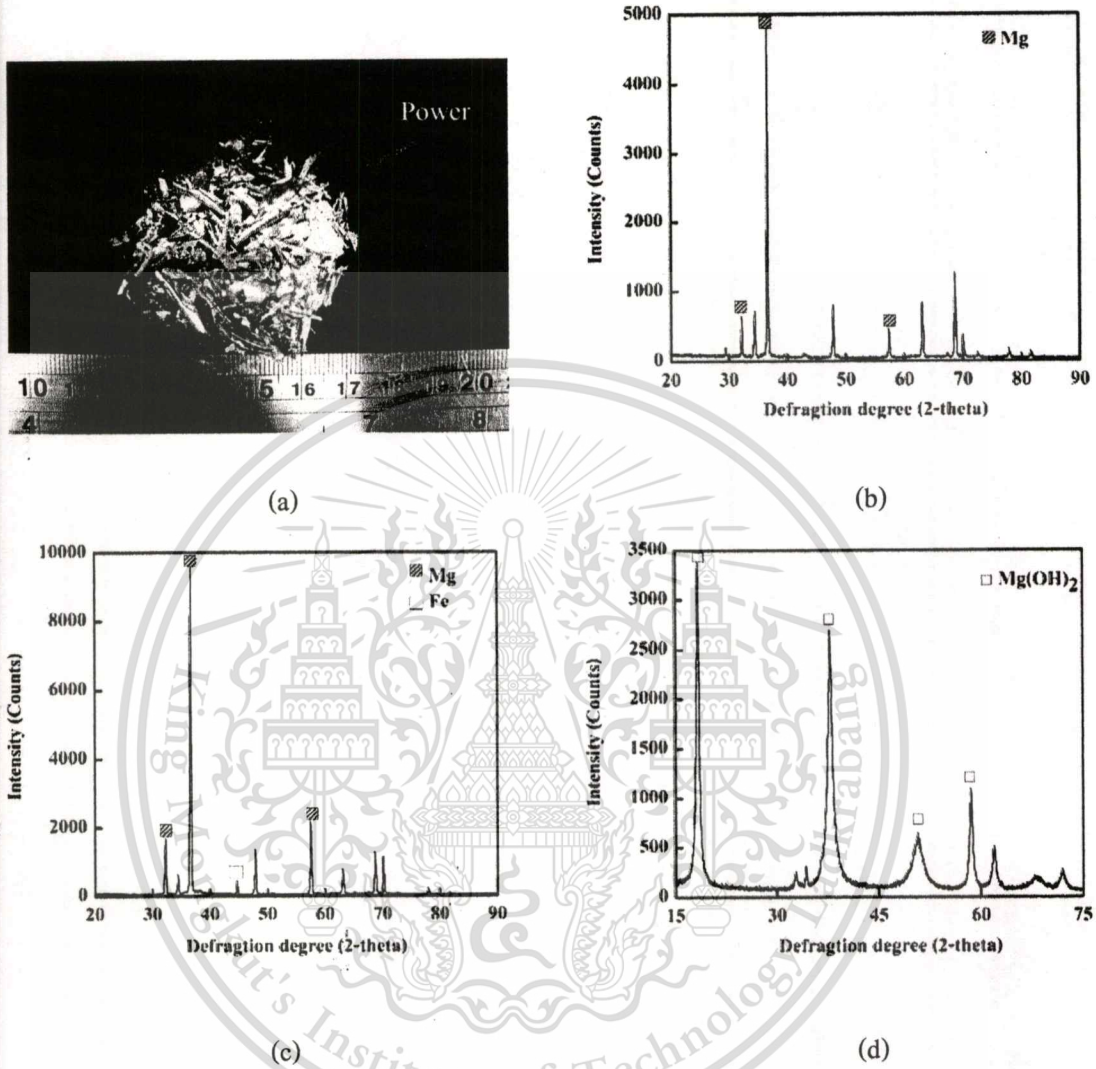

Figure 4.7 External appearance of magnesium scraps after sintering (a) and XRD results of the corresponding magnesium scraps (b) before, (d) after sintering and (c) unknown powder after sintering

4.1.5 SEM and EDS results

4.1.5.1 Relative Oxygen Content

Takahashi suggested a method to measure the percentage of oxide by relative oxygen, which came from the effect of moisture or oxygen contain in atmosphere after sintering, by using the SEM and EDS analysis the element from the specimens and using the **equation 3.10** for calculation. The oxygen per aluminium contents measured at the centre of the specimens that were sintered in 99.5% purity of nitrogen. The results from the element analysed by EDS are shown in **Table 4.1.** The results after calculation show that condition without and with were 0.107 and 0.12 which is different from the green specimens. By comparing with their green stage, it was found that oxygen content observed on the sintered specimens were increased for the specimens sintered in condition without and with Mg sacrificial. The results show good agreement with a better sinterability in condition without sacrificial Mg, which show a lower relative oxygen content. However, from the sacrificial Mg condition was no evidence of reduction by nitrogen as shown in Liu *et al.*, 2008.

Table 4.1 Percentage of element measured by EDS from sintered specimens with 99.5% purity of nitrogen

Element	Green sample (% weight)	Sintered without Mg (% weight)	Sintered with Mg (% weight)
Oxygen (O)	**2.53**	2.1	2.53
Magnesium (Mg)	**0.59**	1.35	1.13
Aluminium (Al)	**67.77**	38.24	40.99
Silicon (Si)	**25.67**	55.00	51.24
Iron (Fe)	**-**	0.62	0.75
Copper (Cu)	**1.25**	3.15	3.37
Relative oxygen	**0.07**	0.107	0.12

4.1.5.2 Pore Investigate by EDS Results

SEM and EDS analysis was used to observe the pores, which appeared in the sintered condition with sacrificial magnesium. In micrograph shown that there are still some original pores from the spacing between powder compacted. Area in red circle in **Figure 4.7 (a)** is well sintered and shown clear necking of powder. Therefore, **Figure 4.7 (b)** is the zoom in of poor sintering area within the pore. The EDS results found the trance of iron in pore area as shown in ED results **Figure 4.6 (d)**, this caused the poor sinterability. The iron affected not only on the surface of specimen but also inside the specimen. After the sacrificial magnesium was present, the impurity in sintering condition which caused the poor mechanical and physical properties.

4.2 Effects of Sintering Conditions on Mechanical Properties

4.2.1 Macroscopic Hardness

Figure 4.8 showed the plot of hardness (Hardness Rockwell F-scale) as a functions of time from 1 hour until 5 weeks after sintering with 99.999% purity of nitrogen in condition without sacrificial magnesium. It is noted that, for the apparent hardness increased as a function of times, this was natural age hardening response commonly observed in aluminium P/M alloy (Kent *et al.* (2005) and D.W. Heard *et al.* (2009)). From the graph, the hardness was rose increasing in the first 170 hours or a week after that, the rate of increasing was half. This results show that the suitable selection of period of age hardening is one week after sintered, which will be used for measurement in varied sintering atmosphere conditions in this works.

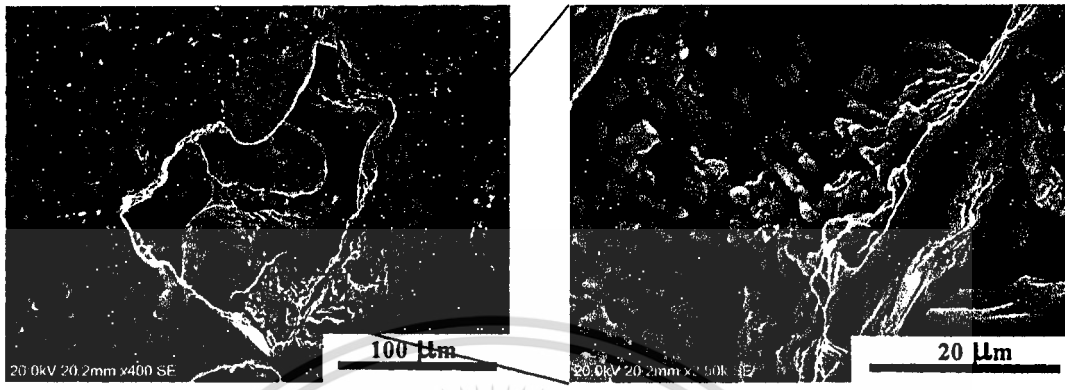

(a) (b)

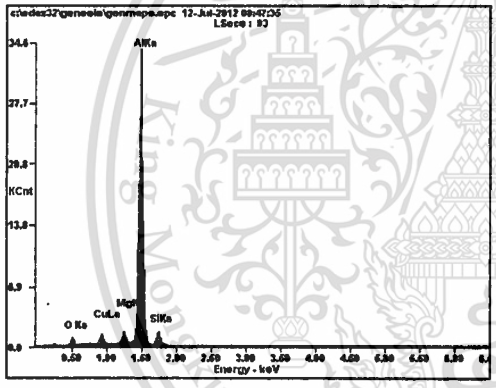

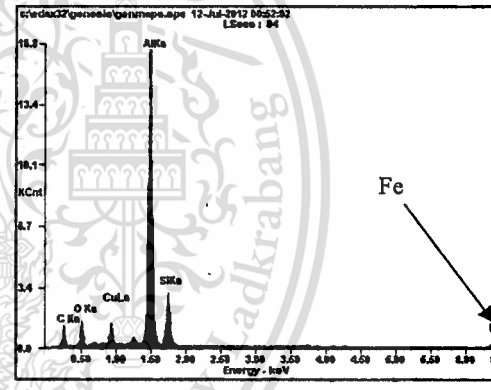

Element	*Wt%*	*At%*
OK	05.56	09.27
CuL	04.77	02.00
MgK	02.68	02.95
AlK	78.68	77.87
SiK	08.31	07.90
Matrix	Correction	ZAF

Element	*Wt%*	*At%*
CK	20.35	36.49
OK	10.37	13.95
CuL	07.39	02.50
AlK	45.44	36.27
SiK	11.62	08.91
FeK	04.84	01.87
Matrix	Correction	ZAF

(c) (d)

Figure 4.7 Scanning electron micrograph (SEM) of specimens sintered using 99.5% purity of nitrogen with sacrificial magnesium (a) area surrounded a large pore and (b) zoom in of poor sintering area within the pore, and (c) and (d) corresponding EDS results respectively

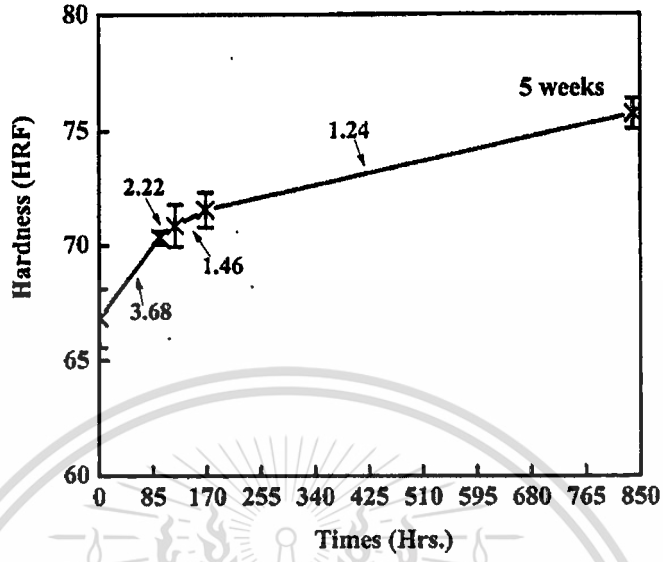

Figure 4.8 Artificial age hardening showing the hardness in Rockwell scale F as a function of time for specimen sintered using 99.999% purity of nitrogen without sacrificial magnesium

After the waiting time for hardness test due to natural age hardening was selected, the appearance hardness between surface and center of specimens was investigated and shown in **Figure 4.9**. The hardness was measured in the condition without and with sacrificial magnesium by using 99.999% purity of nitrogen. The hardness of the specimen at the surface for the conditions without and with sacrificial are 70.4 and 70.3 HRF. The hardness at centre of specimens showed no significant different to that surface, which are 73.0 and 72.3 HRF for without and with sacrificial magnesium respectively. From the results, in subsequent experiment of varied conditions of sintering with purity of nitrogen and without or with sacrificial magnesium, only hardness at the surface was measured.

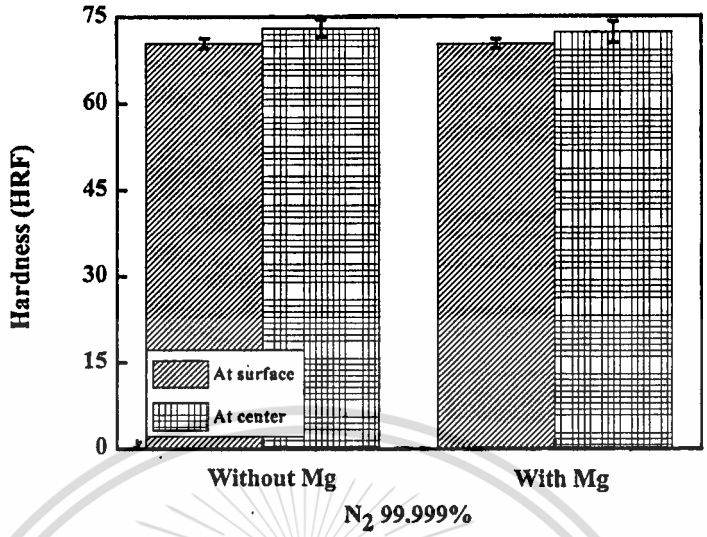

Figure 4.9 Hardness in Rockwell scale F measured at the center and surface of specimens sintered using 99.999% purity of nitrogen without and with sacrificial magnesium

Figure 4.10 shows the macroscopic hardness results of specimen with a different sintering conditions. The hardness without sacrificial magnesium, showed that the results was increased a little with higher purity of nitrogen. On the other hand, the present of sacrificial Mg condition shown poor sinterability, which compared with the same purity.

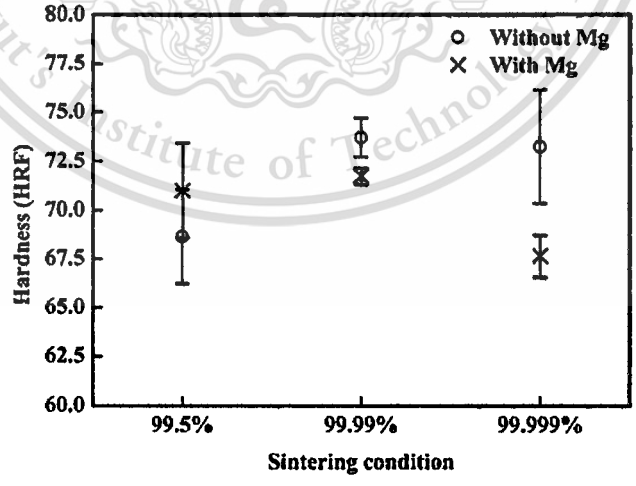

Figure 4.10 Hardness in Rockwell scale F for specimens sintered using different conditions

4.2.2 Tensile Properties

In addition, the corresponding tensile strength and elongation of sintered specimens are illustrated in **Figure 4.11 (a)** and **(b)**. The tensile properties had similar trend as the density and hardness. This results can supported by microstructure of sample sintering without and with sacrificial magnesium from the sample sintered with 99.5% of nitrogen. The value were obtained from the specimens condition without sacrificial magnesium, which were 137.8, 158.3 and 148.5 MPa for tensile strength and 2.48, 2.71 and 2.51 % for elongation along the purity of nitrogen with 99.5, 99.99 and 99.999 %. And for the sintering with sacrificial magnesium the value were 123.3, 129.9 and 120.8 MPa for tensile strength and 1.69, 1.69 and 1.27 % for elongation.

According to the tensile properties, it show that the results can divided into two main groups which are sintering without and with sacrificial magnesium. As the effect from the purity has less effect to the results of mechanical and physical properties. The defect of iron that found after used magnesium to scarified condition supported by EDS and XRD results which made the specimens have poor sintering results.

4.3 Experiment Conclusion

In summary, the purity of nitrogen has no significant results to the properties of the sinterability. Therefore, the present of the sacrificial Mg show the opposite results, which is the poor sinterability can be observed. The suitable sintering condition for Al-Si alloy is using 99.5% purity of nitrogen atmosphere and without sacrificial Mg. The formation of AlN was interrupted by used the sacrificial magnesium condition.

The present of magnesium did not improve the mechanical properties because the formation of AlN was interrupted by adding magnesium scrap. The formation of AlN can observed from XRD results. The XRD results that sintering without sacrificial magnesium condition has more AlN formation than sintering with sacrificial magnesium. The formation of AlN has an importance role, which can improve the densification in the sintering of aluminium. The formation of AlN can reduce the pressure in the pore space (Schaffer *et al.*, 2006). The increasing formation of AlN can increase sintered density, which can also improve the physical and mechanical properties. Hence, less

formation of AlN when sintering with magnesium resulted in sintered sampled with lower density and poorer physical and mechanical properties.

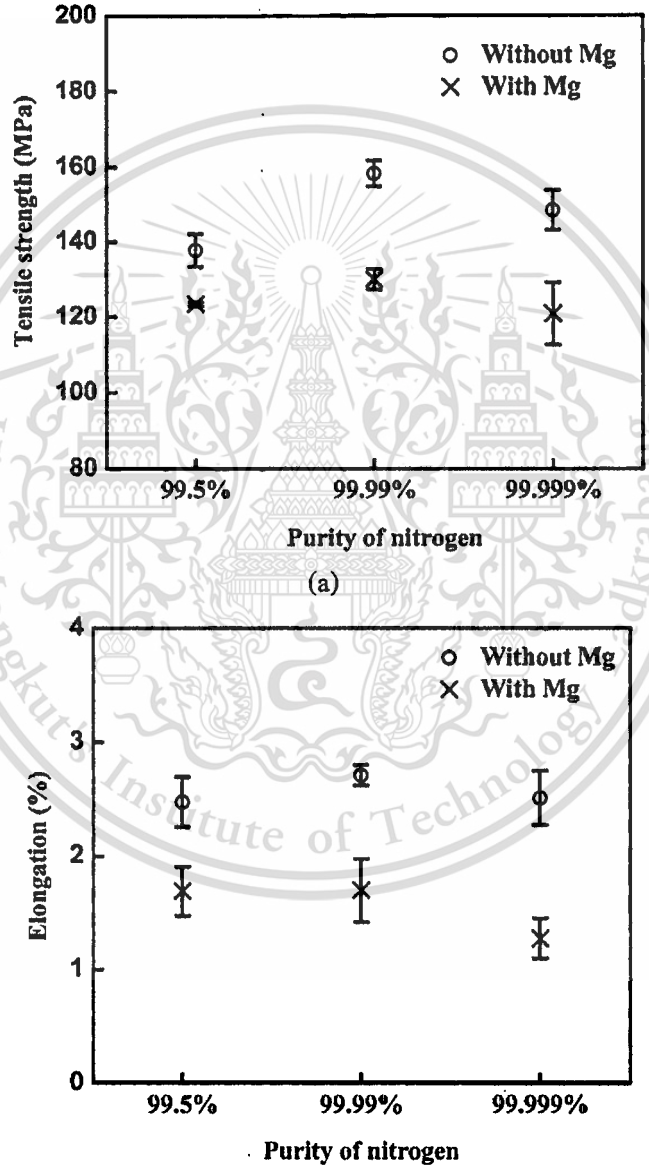

Figure 4.11 (a) Tensile strength and (b) elongation of specimens sintered using different conditions.

CHAPTER 5

INJECTION MOULDING OF AL-SI ALLOY POWDER IN AUTOMOTIVE PARTS

From the previous chapter, the experiments identified the suitable condition for sintering Al-Si alloy, which is the sintering with temperature of 560°C for 1 hour under 99.5% purity of nitrogen without sacrificial magnesium. As a results, this sintering condition will be adapt to use for aluminium injection moulding in this chapter. The experiments can be divided into two main parts based on the type of binders. The first part utilised the self-mixed binder components, which contains polypropylene (PP), paraffin wax (PW), and stearic acid (SA). All components can be supplied from the local suppliers. The second part utilised the commercial binder from Mold Research Co.,Ltd., Japan, which is polyacetal based binder. The commercial binder is imported (Kankawa 1998).

The green specimens were sintered by using the suitable sintering obtain from the first experiment.

5.1 Differential Scanning Calorimetry (DSC) and Thermogravimetric Analysis (TGA) Results

Considering the self-mixed binder components in **Table 5.1,** polypropylene has the highest melting temperature, which is 175°C. While, the melting points of paraffin wax and stearic acid are significant lower at 60°C and 55°C respectively. To ensure that all components were melted during mixing, the mixing was carried out at 180°C. However, it is noted that the decomposition of stearic acid starts at 170°C from the TGA result. It was likely that some stearic were decomposed but the rate of decomposition is relatively slow as shown in **Appendix B.** The TGA results of

polypropylene, paraffin wax and stearic acid shown that they were decomposed at different temperatures ranging between 170-540°C under oxygen atmosphere.

The commercial binder MRM was tested using two different atmospheres, which are under oxygen (O_2) and nitrogen (N_2). The results show little difference of melting point temperature as can be seen in **Appendix B1-B2.** The DSC results show the several peaks of melting temperature; this confirm that the MRM polyacetal based binder was blend and mixed with another polymer. The highest melting peak temperature is at 157°C for oxygen atmosphere, which can be applied to used for setting the mixing temperature. The effect of atmosphere on the thermal debinding are evident in TGA results. Under oxygen atmosphere, the decomposition starts and ends at 183°C and 530°C respectively. However, under nitrogen atmosphere the decomposition starts and ends at 130°C and 550°C respectively. The commercial binder was decomposed under a wider temperature range for nitrogen atmosphere.

Table 5.1 The results of differential scanning calorimetry (DSC) and thermogravimetric analysis (TGA) techniques for binder

Binder	Testing atmosphere	DSC Temperature (°C)	Decomposed Range Temperature (°C)
Polypropylene	O_2	175	350-510
Paraffin wax		60	205-540
Stearic acid		55	170-525
Commercial (MRM)	O_2	157	185-530
	N_2	160	130-550

5.2 Effects of Debinding and Sintering Process on Aluminium Metal Injection Moulding

5.2.1 Effect of Debinding and Sintering Processes using Self-Mixed Binder

The green specimens with various formulation conditions and the results of debinding included sintering are shown in **Table 5.1.** It shows that the green density was varied with solid loading, pressure, and moulding temperature, which were used to formed the green specimens. The solid loading influences the quantity of binder contained in the feedstock. The lower solid loading need higher mould temperature of 100°C. This contains more binder in feedstock and some of binder was leaked from the mould. When it cooled down, the green specimen was different to remove. In case of the increased pressing pressure with constant temperature at 80°C. This needs to make the intermetallic connected between the aluminium powder that covered with binder. Green parts were then thermally debinded at 400°C for 1 hour in air. The brown specimens were shown in **Figure 5.1.** All conditions shown the good appearance with gray-light colour without crack. However, the 51.9% solid loading condition (e) was measured the weight. This cause an error which cannot measured the binder loss. In case of the same solid loading at 56.5% (a) and (b), the higher temperature of moulding show more percentage of binder loss. The moulding processed has already made some binder loss along the moulding process. While, the same condition with the same temperature of moulding with different compact pressured show no significant effect to the percentage of binder.

All brown specimens from debinding were transferred to a new setter and sintered with 560°C for one hour in nitrogen atmosphere with 99.99% purity of nitrogen as shown in **Figure 5.2.** The sintered specimens with different binder formulation conditions show the different appearance compared with green specimen [**Figure 5.2 (a)**]. The sintered specimens changed to the dark brown colour. The 54.8% solid loading (d) shows the explode effect. This results from the rate of temperature raised for sintered was not suitable for this solid loading. All sintered specimens still had the binder remained within the specimens that can measured and calculated the percentage binder loss

after sintering as shown in the **Table 5.2.** From the calculation percentage binder lose after sintered, there were still 21-25% binder remained within the sample. Hence, the sintering was unsuccessful.

Table 5.2 The different binder formulation conditions

Conditions	Solid loading (%)	Moulded Temperature (°C)	Compaction Pressure (MPa)	Green weight (g)	Green density (g/cm^3)	Brown weight (g)	Debinded Binder loss (%)	Sintered weight (g)	Sintered Binder loss (%)
(a)	56.5	80	140	2.009	1.829	1.653	33.1	1.668	79.67
(b)			100	1.989	1.673	1.678	28.91	1.640	81.53
(c)		180	140	1.717	2.098	1.454	58.96	1.440	75.27
(d)	54.8			1.748	1.860	1.442	74.2	*	*
(e)	51.9			1.983	1.860	*	*	*	*

* Cracks, Surface cracks, Explodes

Figure 5.1 Self-mixed binder specimens after debinded using air atmosphere

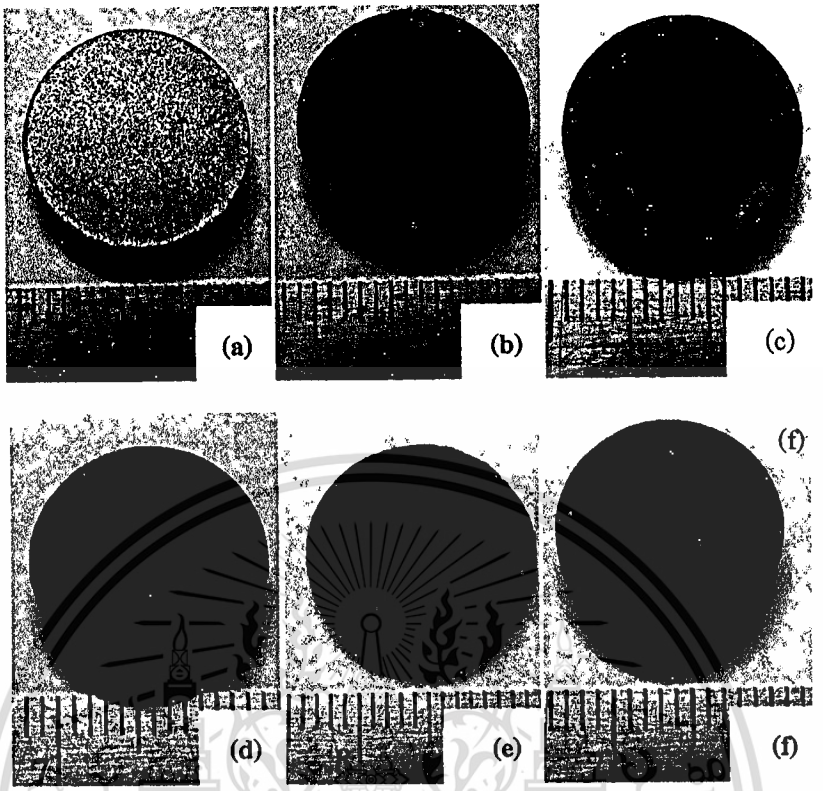

Figure 5.2 Green parts and sintered parts using self-mixed binder which (a) green specimen, (b) 56.5% with 80°C 140 MPa, (c) 56.5 % with 80°C 100 MPa, (d) 56.5% with 100°C, (e) 54.8%, and (f) 51.9%

5.2.2 Effects of Debinding and Sintering Processes using Commercial Binder

The commercial MRM binder was composed of a number of different kinds of polymers as evident from DSC and TGA results, which included in **Appendix B-4**. Binder burnout is inherent to final debinding which was affected by the temperature and atmosphere. In this experiment, the parameter which were concerned are the temperature and atmosphere.

5.2.2.1 Effects of Thermally Debinding in Air

An air debinding furnace is the commercial furnace which is commonly used for debinding the binder from MIM parts. Air is commonly applied for the commercial debinding process because it economical. The conditions, which used to test for commercial binder specimens, are shown in **Table 5.3.** The specimens were injection moulded into the tensile test bar shape. The average green specimen was 1.80 g/cm^2. Green specimens were debinded at 260°C and

340°C for 2 hours. The debinded specimens had the same appearance with gray and light brown colour. Both conditions showed no defect, without cracks and blister on the specimens. The results from debinding atmosphere at 340°C has 99.75% of binder. Specimen debinded at lower temperature 260°C showed lower percentage of binder loss 80.68%. Within the same holding time, the temperature has effect on the debinded rate. However, the effect of oxidation from the oxygen and moisture contain in the air need to improved by using the nitrogen atmosphere, which is shown more in detail by next section.

Table 5.3 The thermal debinding condition and debinded results which appeared in this experiments

Conditions	Green weight (g)	Brown parts weight (g)	Debinding Extraction (%)
260°C	4.967 ± 0.01	4.034 ± 0.01	80.68 ± 0.5
340°C	4.977 ± 0.01	3.818 ± 0.01	99.75 ± 0.9

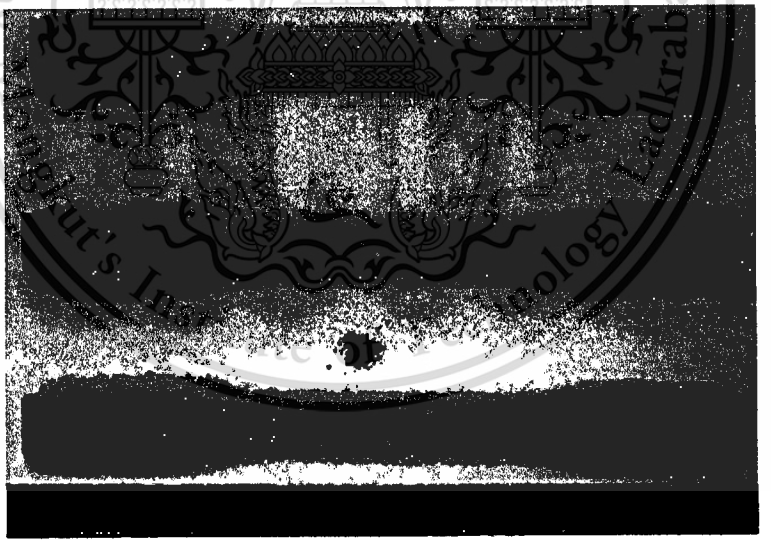

Figure 5.3 Debinded specimens with thermally using 340°C for 2 hours under air atmosphere

5.2.2.2 Effects of Thermal Debinded in Nitrogen

From the TGA results shown in **Appendix B-6,** to burnout the MRM binder in nitrogen atmosphere needs higher temperature. This is also observed in German and Bose, 1997. Green parts were thermally debinded using different debinding temperature and time as shown in **Table 5.4.** The results shown that as the debinding temperature increased, the percentage of binder loss increased. Similarly, the debinding time increased, the percentage of binder loss also increased. The results shown that the same debinding pattern from debinding under air conditions cannot be used for debinding under nitrogen atmosphere. Heard *et al.*,(2009) show that the liquid phase sintering (LPS) from was started from 420°C. The nitrogen atmosphere needs higher temperature and longer times for debinded. In case of higher temperature near the primary rearrangement phase of LPS, the binder was still inside. This caused the poor sinterability.

Table 5.4 Percentage binder loss after debinding using different thermal debinding temperature and time

Conditions	Times (hrs.)	Green weight (g)	Brown weight (g)	Debinding Extraction (%)
340 °C	2	4.968 ± 0.01	4.082 ± 0.01	67 ± 1.3
340 °C	3	4.984 ± 0.04	3.983 ± 0.01	89.13 ± 0.2
450 °C	2	5.035 ± 0.003	3.77 ± 0.004	96.0 ± 0.2
450 °C	3	4.979 ± 0.02	3.735 ± 0.02	98.2 ± 0.4

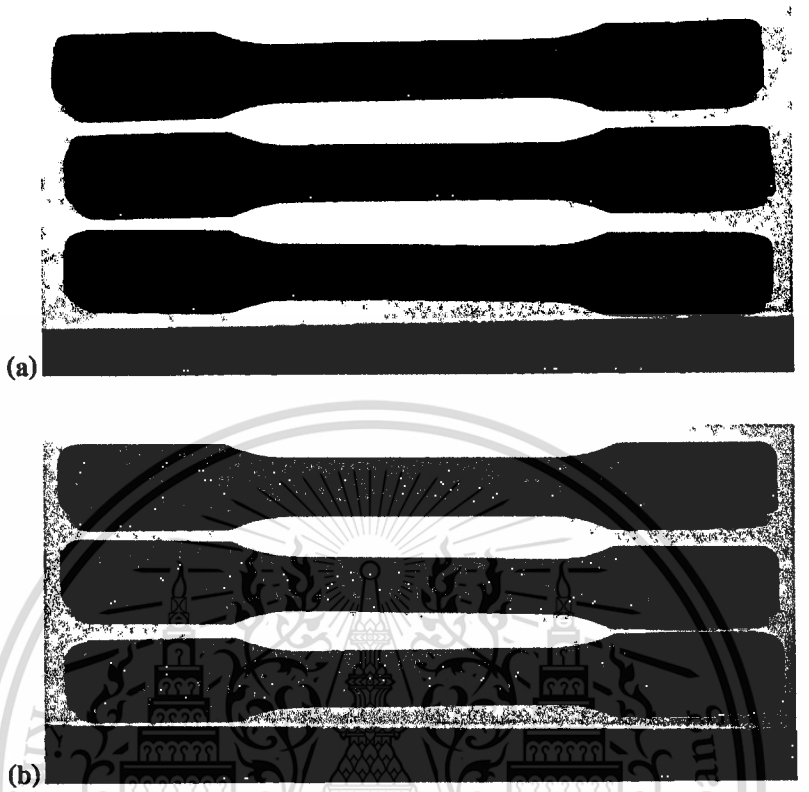

Figure 5.4 Brown specimens debinded using (a) 340°C and (b) 450°C debinding temperature in nitrogen atmosphere

5.2.2.3 The Effect of Solvent and Thermal Debinding in Nitrogen

In this experiment, the solvent debinding was applied to the specimens before thermal debinding solvent debinding was used to dissolve some component, which contain in commercial binder. Subsequently, the binder inside the specimen can be extracted by the thermal debinding with the faster rate of heating and reducing thermal debinding time. The results of solvent debinding using hexane at 40°C for 4 hours and 8 hours were shown in **Table5.4.** Subsequently, the thermal debinding at 400°C for 2 hours and sintering at 560°C for 1 hour with 99.5 percentage purity of nitrogen.

The results show that doubling the solvent debinding times does not double the percentage of binder loss. However, the percentage of binder loss increases from 29% to 43% after the solvent debinding, time was increased from 4 hours to 8 hours. On the other hand, the percentage binder loss after sintering were both about 94% and 99%. This can suggest that most binder will be removed during sintering, hence the thermal debinding rate can be increased.

Table 5.4 Solvent debinded and sintered results under nitrogen atmosphere

Conditions	Green weight (g)	Solvent debinded weight (g)	Debinding Extraction (%)	Thermal debinded and sintered weight (g)	Sintered Extraction (%)
(a) 4 Hrs.	4.969 ± 0.01	4.591 ± 0.02	29.14 ± 1.67	3.7452 ± 0.01	94.39 ± 0.2
(b) 8 Hrs.	4.971 ± 0.004	4.416 ± 0.004	42.76 ± 0.37	3.685 ± 0.02	99.11 ± 1.4

Figure 5.5 The sintered specimens was shown in this figure after the solvent and thermal debinding

Figure 5.6 shows the XRD results to compare the chemical reaction which are aluminium powder, MRM binder, solvent debinded and sintered specimens. Each XRD result was shown in **Appendix C.** XRD results were shown no significant chemical reaction between Al-Si alloy and binder which can cause the unsuccessful sintering. The intensity of the graph shown only

the reduced peak of paraffin wax which is the MRM component. This shows that the binder was removed by debinding and sintering process.

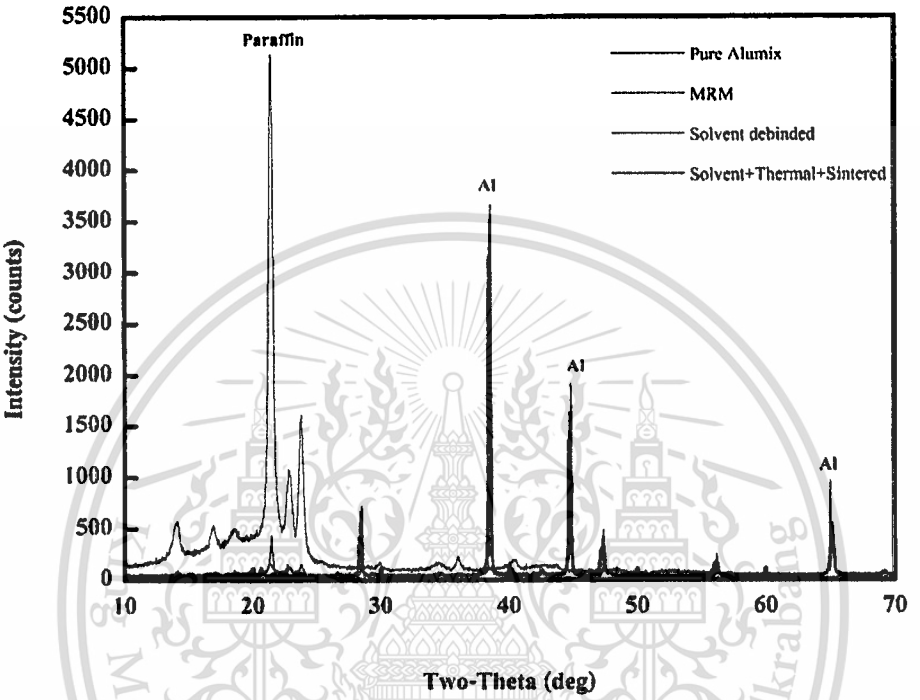

Figure 5.6 Process effects with the XRD results compared between raw materials and debinded specimens

CHAPTER 6

CONCLUSION AND SUGGESTIONS

6.1 Conclusions

6.1.1 Effect of Purity of Nitrogen and Sacrificial Materials on Al-Si Alloy Sinterability.

The suitable condition observed in this experiment was the flow controlled 99.5% purity of nitrogen gas without sacrificial magnesium by using the tube furnace with appropriated 4 l/min flow rate of gas. The dewaxing and sintering temperature were 420°C and 560°C respectively and the sintering time was 60 minutes.

The effect of purity of nitrogen gases shown no significant difference in the properties of sintered specimens when they were sintered using different purity of nitrogen gas. From result of sintered with 99.5% purity of nitrogen without magnesium, the sintered density was 2.61 g/cm^3. The linear shrinkage has no significant difference from the purity of nitrogen effect. However, the sintering with sacrificial magnesium conditions was shown lower shrinkage of specimens. The shrinkage was not uniform because of the nature of specimens that were compacted uniaxially. The microscopic hardness measured at the centre of specimens was 69 HRF after age hardening for 1 week. The tensile strength of 137.8 MPa with 2.48% of elongation could be obtained. The poor sintered surface included pore was appeared in the condition sintered with sacrificial magnesium and also by the microstructure show the poor sinterability with more porosity appeared. However, the better duplex microstructure that consisted of silicon phase dispersed in the aluminium matrix was shown in without sacrificial magnesium conditions. The main factor that influenced the properties was an atmosphere that used to sintered the specimen as the XRD results shown the higher intensity

of AlN. The formation of AlN reduced the pressure in the pore space, inducing pore filling into which can approve the densification. The sacrificial magnesium material was reacted with the oxygen by the XRD results showing the Magnesium hydroxide (Mg (OH_2)) in the used sacrificial magnesium. Therefore, the sacrificial magnesium in this experiment did not improve the sintering atmosphere and also disturb AlN chemical reactions. The sintering of Al-Si-Cu-Mg powder cannot improved by using the sacrificial magnesium scrap and the purity of nitrogen has less effect to the sintereabiliy.

6.1.2 Aluminium Injection Moulding Processes

In the condition with self-mixed binder found that, this formulation which contained with polypropylene (25%), paraffin wax (70%), and stearic acid (5%), is not suitable to use with the Al-Si alloy with the unsuccessful with thermal debinding and sintering with the previous sintering condition. The thermal debinding specimens were exploded and cracked within air condition by using a commercial process of air debinding. The low rate of binder loss was appeared which is not sufficient. The commercial binder (MRM) which is a polyacetal-based binder was successful moulded into tensile specimens using the injection pressure of 80 MPa, the moulding temperature of 45°C, the injection temperature of 175°C, and the injection time 5 minutes.

The successful debinding condition for tensile specimen which is the combined solvent and thermal debinding. The solvent debinding with hexane was obtained with temperature at 40°C for 8 hours. The percentage of binder loss from solvent debinding is 43%. Then, the thermal debinding under nitrogen atmosphere was applied to the specimens with temperature at 400°C holding for 2 hours. The percentage of binder loss become 99%. Therefore, the sintering condition from first parts cannot use for sintering with this brown parts which the results show unsuccessful with sintered specimens. XRD results show evidence that will be affected from raw material until the specimens have sintered. XRD shown only the intensity of binder was decreased.

6.2 Suggestion

This is the first step for the Al MIM using the commercial process. There are some suggestions to the work for further study as follow:

6.2.1 Study the sintering aids which could be affected to improve the sinterablility.

6.2.2 Study further about the improving the hardness after sintering.

6.2.3 Study the binder formulation and binder composition.

6.2.4 Study debinding parameter such as debinding technique, debinding atmosphere debinding rate.

6.2.5 Study the real time chemical reaction changing.

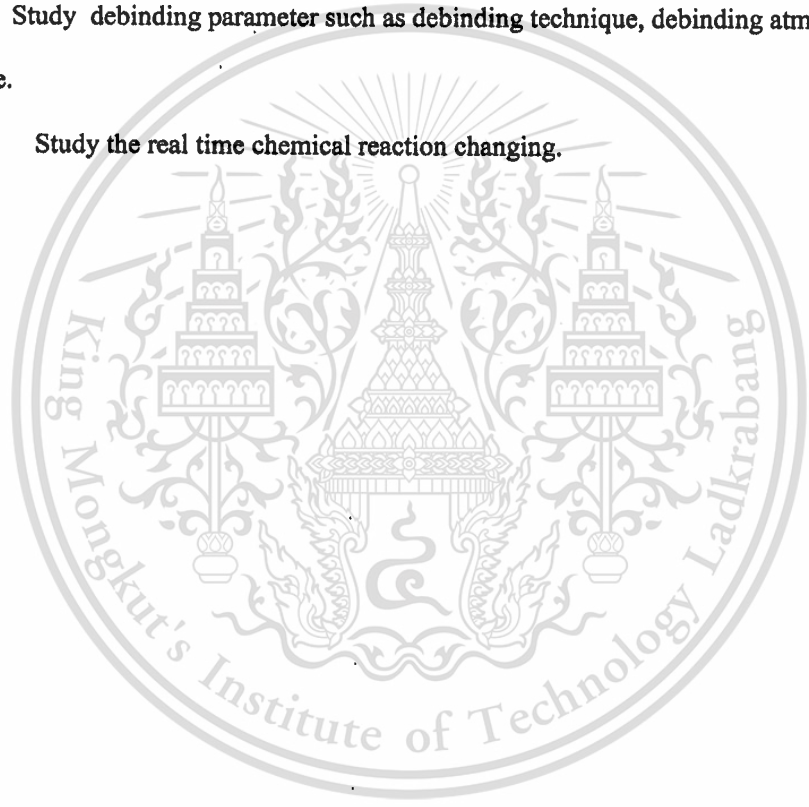

REFFERENCE

1. A. Salee, A. Manonukul, C. Thianpong, and K. Takahashi. "Improving Sinterability of Aluminium Alloy (Al-Si-Cu-Mg) by Adjusting Sintering Conditions." **Proceeding of the 2nd Thammasat University International Conference on Chemical, Environmental and Energy Engineering**, Bangkok, Thailand, March 3-4, 2009. 226-231.
2. Andreeva, N.G., Rastrigina, E.F. 1966. "Theory and Technology of Sintering, Heat Treatment, and Chemiothermal Treatment Process Mechanism of Metallic Contact Formation in SAP Type Alloys." Translated from **Poroshkovaya Metallurgiya.** 3 (39): 27-36.
3. ASM International. 2004. **ASM Handbook of Powder Metallurgy.** 7: 381-385.
4. ASTM International. 2005. **Annual Book of ASTM Standards: Metallic and Inorganic Coatings; Metal Powders, Sintered P/M Structural Parts.** Vol. 02.05. Pennsylvania : ASTM International.
5. Fuentes, J.J., Rodriguez, J.A., Herrera, E.J. 2003. "Effect of Mg as Sintering Additive on the Consolidation of Mechanically Alloyed Al Powder." **Materials Science Forum.** 426-432: 4331-4336.
6. German, R.M. 1994. **Powder Metallurgy Science.** 2nd ed. New Jersey: Metal Powder Industries Federation.
7. German, R.M. 1996. **Sintering Theory and Practice.** New York: John Wiley and Sons.
8. German, R.M., Bose, A. 1997. **Injection Molding of Metals and Ceramics.** New Jersey: Metal Powder Industries Federation.
9. Gutin, S.S., Panov, A.A., Khlopin, M.I. 1972. "Effect of Oxide Films in the Sintering of Aluminium Powders." Translated from **Poroshkovaya Metallurgiya.** 112 (4): 32-35.

REFFERENCES (CONT.)

10. Heard D.W., Donaldson I.W., Bishop D.P., 2009 "Metallurgical Assessment of Hypereutectic Aluminum-Silicon P/M Alloy." **Journal of Materials Processing Technology.** 209 5902-5911.

11. Hunt Jr. H.W., 1998 "Metallurgical Considerations in the Design and Processing of Aluminum Powder Metallurgy Alloy" **Powder Metallurgy Aluminum and Light Alloys for Automotive Applications Conference.** 1-9.

12. Kimura, A., Kondoh, K., Shibata, M., Watanabe, R. 2001. "Breakaway Behavior of Surface Oxide Film on Aluminium-Silicon-Magnesium Alloy Powder Particles at High Temperature in Vacuum." **Materials Transactions.** 42 (7): 1373-1379.

13. Krajnikov, A.V., Gastel, M., Ortner, H.M., Likutin, V.V. 2002. "Surface Chemistry of Water Atomised Aluminium Alloy Powders." **Applied Surface Science.** 195: 26-43.

14. Liu, Z.Y., Sercombe, T.B., Schaffer, G.B. 2008. "Metal Injection Moulding of Aluminium Alloy 6061 with Tin." **Powder Metallurgy.** 51 (1): 78-83.

15. Lui, Z.Y., Kent D., Schaffer, G.B. 2009. "Powder Injection Moulding of an Al-AlN Metal Matrix Composite." **Material Science and Engineering.** 513 (14): 352-356.

16. Lumley, R.N., Sercombe, T.B., Schaffer, G.B. 1999. "Surface Oxide and the Role of Magnesium During Sintering of Aluminium." **Metallurgical and Materials Transactions.** 30A: 457-463.

17. Lutgens, F.K., Tarbuck, E.J. 1998. **The Atmosphere: An Introduction to Meteology.** 7th ed. New Jersey, Prentice-Hall International: 77-84.

18. MacAskill I.A., Hecemer R.I., Donaldson I.W., Bishop D.P. 2010 "Effect of Magnesium, Tin and Nitrogen on the Sintering responde of Aluminum powder." **Journal of Materials Processing Technology.** 210: 2252-2260.

REFFERENCES (CONT.)

19. McLeod, A.D., Gabryel, C.M. 1992. "Kinetics of the Growth of Spinel, $MgAl_2O_4$, on Alumina Particulate in Aluminium Alloys Containing Magnesium." **Metallurgical Transactions.** 23A: 1279-1283.

20. Metal Powder Industries Federation. 2002. **Standard Test Methods for Metal Powders and Powder Metallurgy Products.** New Jersey: Metal Powder Industries Federation.

21. Nicolas P. 1998. **Advanced Polymer Processing Operation.** 213-277.

22. Nishiyabu, K., Matsuzaki, S., Ishida, M., Tanaka, S., Nagai, H. 2004. "Development of Porous Aluminium by Metal Injection Moulding." **Materials Forum.** 28: 376-382.

23. Pieczonka, T., Schubert, Th., Baunack, S., Kieback, B. 2007. "Dimensional Behavior of Aluminium Sintered in Different Atmospheres." **Materials Science and Engineering.** A: 1-6.

24. Schaffer, G.B. 2004. "Powder Processed Aluminium Alloys." 65-74. In Nie, J.F., Morton, A.J., Muddle, B.C. **Materials Forum.** 28: Institute of Materials Engineering Australasia Ltd.

25. Schaffer, G.B., Hall, B.J. 2002. "The Influence of the Atmosphere on the Sintering of Aluminium." **Metallurgical and Materials Transactions.** 33A: 3279-3284.

26. Schaffer, G.B., Hall, B.J., Bonner, S.J., Hou, S.H., Sercombe, T.B. 2006. "The Effects of the Atmosphere and the Role of Pore Filling on the Sintering of Aluminium." **Acta Materialia.** 54: 131-138.

27. Schaffer, G.B., Sercombe, T.B., Lumley, R.N. 2001. "Liquid Phase Sintering of Aluminium Alloys." **Materials Chemistry and Physics.** 67: 85-91.

28. Sercombe, T.B. 1998. "Non-Conventional Sintered Aluminium Alloys." Ph.D. Thesis of The University of Queensland.

REFFERENCES (CONT.)

29. Showaiter, N., Youseffi, M. 2007. "Compaction, Sintering and Mechanical Properties of Elemental 6061 Al Powder with and without Sintering Aids." **Materials and Design**: 1-11.

30. Supati R., Loh N.H., Khor K.A., Tor S.B. 2000. "Mixing and Characterization of Feedstock for Powder Injection Moulding." **Material Letters** 46: 109-114.

31. Takahashi, K., interviewed on September 15, 2008. **Oxide Analysis by Using SEM and EDS Analysis**. The Office of Tokyo Institute of Technology in Thailand.

32. Tan L. K., Ma J. 2004 "Performance of Poweder Injection Molding (PIM) Heat Sink." **Inter Society Conference on Thermal Phenomena**

33. Vukcevic, M., Delijic, K. 2002. "Some New Directions in Aluminium-Based PM Materials for Automotive Applications." **Materiali In Tehnologije**. 36 (3-4): 101-105.

34. Xie, G., Ohashi, O., Song, M., Mitsuishi, K., Furuya, K. 2005. "Reduction Mechanism of Surface Oxide Films and Characterization of Formations on Pulse Electric-Current Sintered Al-Mg Alloy Powders." **Applied Surface Science**. 241: 102-106.

35. Yilmaz, M., Altintas, S. 1996. "Production of Hypereutectic Al-Si Alloys by P/M Route." **Material Science Forum**. 217-222: 1853-1858.

36. Youseffi, M., Showaiter, N., Martyn, M.T. 2006. "Sintering and Mechanical Properties of Prealloyed 6061 Al Powder with and without Common Lubricants and Sintering Aids." **Powder Metallurgy**. 49 (1): 86-95.

APPENDIX

APPENDIX A

MATERIAL AND PROCESSING INFORMATION

Appendix A-1: Product information of ECKA Alumix 231

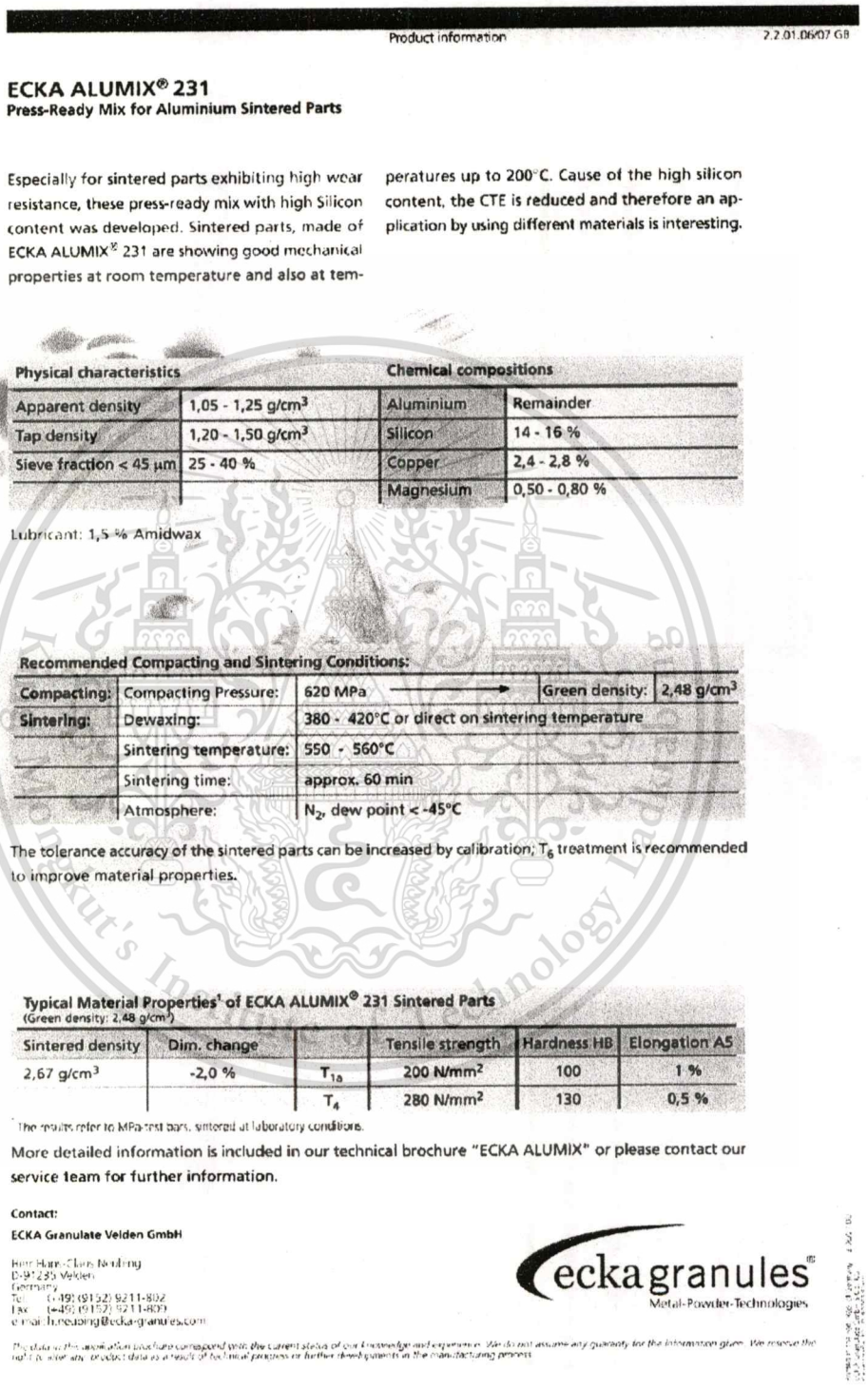

Product information 2.2.01.0607 GB

ECKA ALUMIX® 231
Press-Ready Mix for Aluminium Sintered Parts

Especially for sintered parts exhibiting high wear resistance, these press-ready mix with high Silicon content was developed. Sintered parts, made of ECKA ALUMIX® 231 are showing good mechanical properties at room temperature and also at temperatures up to 200°C. Cause of the high silicon content, the CTE is reduced and therefore an application by using different materials is interesting.

Physical characteristics		Chemical compositions	
Apparent density	1,05 - 1,25 g/cm³	Aluminium	Remainder
Tap density	1,20 - 1,50 g/cm³	Silicon	14 - 16 %
Sieve fraction < 45 µm	25 - 40 %	Copper	2,4 - 2,8 %
		Magnesium	0,50 - 0,80 %

Lubricant: 1,5 % Amidwax

Recommended Compacting and Sintering Conditions:

Compacting:	Compacting Pressure:	620 MPa →	Green density:	2,48 g/cm³
Sintering:	Dewaxing:	380 - 420°C or direct on sintering temperature		
	Sintering temperature:	550 - 560°C		
	Sintering time:	approx. 60 min		
	Atmosphere:	N_2, dew point < -45°C		

The tolerance accuracy of the sintered parts can be increased by calibration; T_6 treatment is recommended to improve material properties.

Typical Material Properties[1] of ECKA ALUMIX® 231 Sintered Parts
(Green density: 2,48 g/cm³)

Sintered density	Dim. change		Tensile strength	Hardness HB	Elongation A5
2,67 g/cm³	-2,0 %	T_{1a}	200 N/mm²	100	1 %
		T_4	280 N/mm²	130	0,5 %

[1] The results refer to MPA-test bars, sintered at laboratory conditions.

More detailed information is included in our technical brochure "ECKA ALUMIX" or please contact our service team for further information.

Contact:
ECKA Granulate Velden GmbH

Herr Hans-Claus Neubing
D-91235 Velden
Germany
Tel. (+49) (9152) 9211-802
Fax (+49) (9152) 9211-809
e-mail: h.neubing@ecka-granules.com

ecka granules®
Metal-Powder-Technologies

Figure A-1 Scanned image of product information of aluminium alloy powder used in this study.

APPENDIX B

DSC AND TGA RESULTS AND INFORMATION

Appendix B-1: DSC results of polypropylene 3342 M

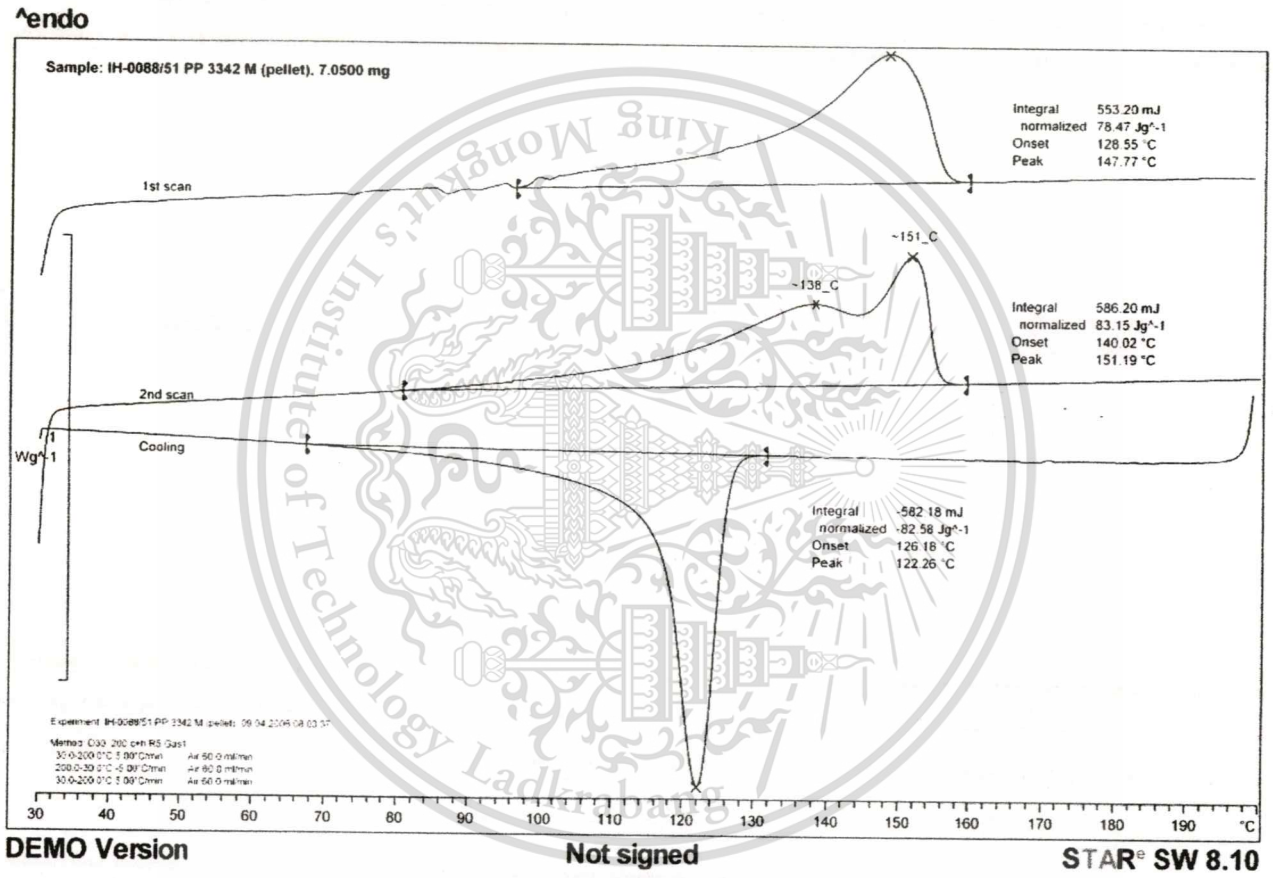

Figure B-1 Scanned image of DSC of polypropylene 3342 M under oxygen atmosphere

Appendix B-2: DSC results of paraffin wax under nitrogen atmosphere

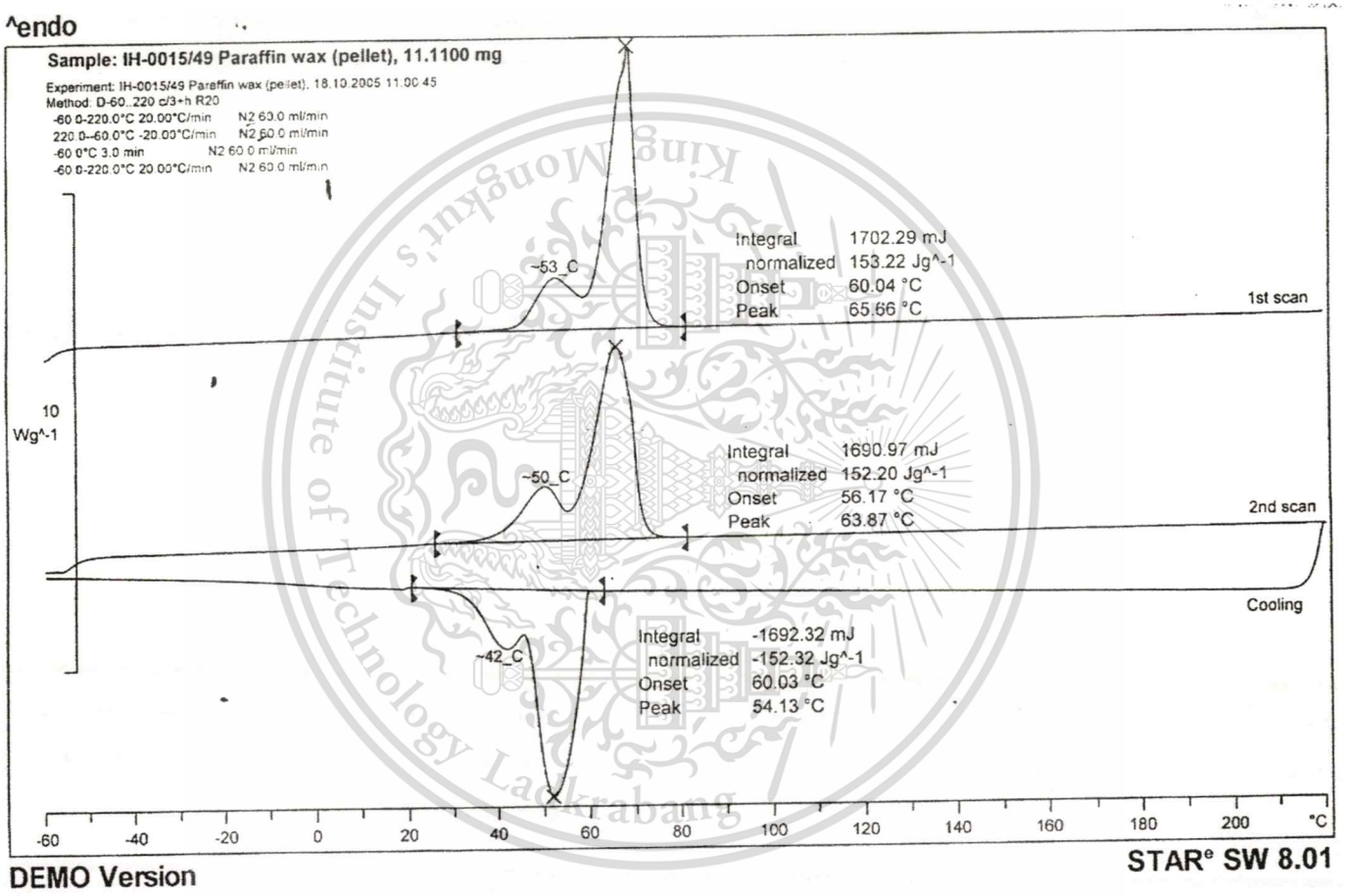

Figure B-2 Scanned image of DSC of paraffin wax under nitrogen atmosphere

Appendix B-3: DSC results of stearic acid

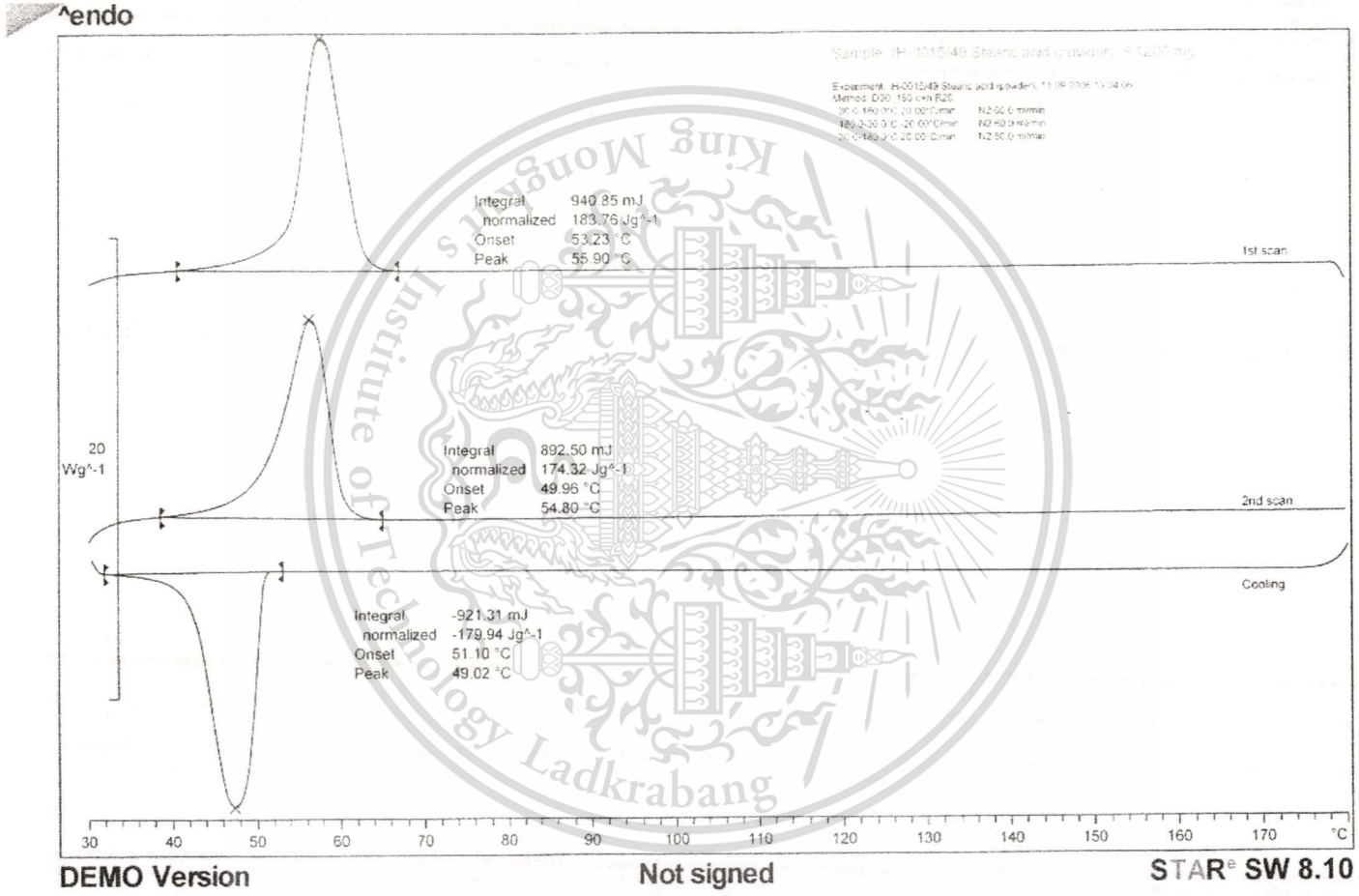

Figure B-3 Scanned image of DSC of stearic acid under nitrogen atmosphere

Appendix B-4: DSC results of commercial binder (MRM)

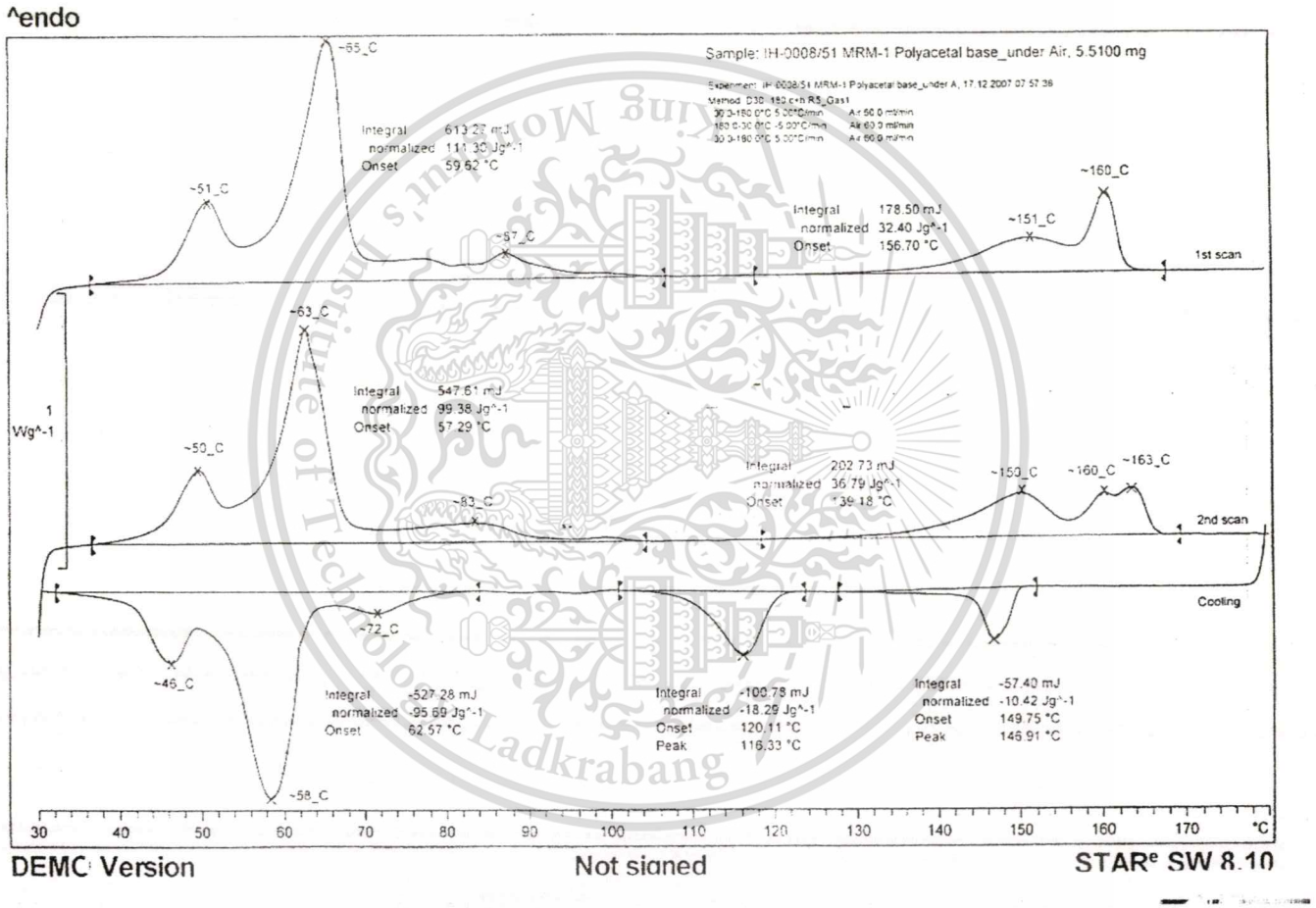

Figure B-4 Scanned image of DSC of commercial binder (MRM) under oxygen atmosphere

Appendix B-5: DSC results of commercial binder (MRM)

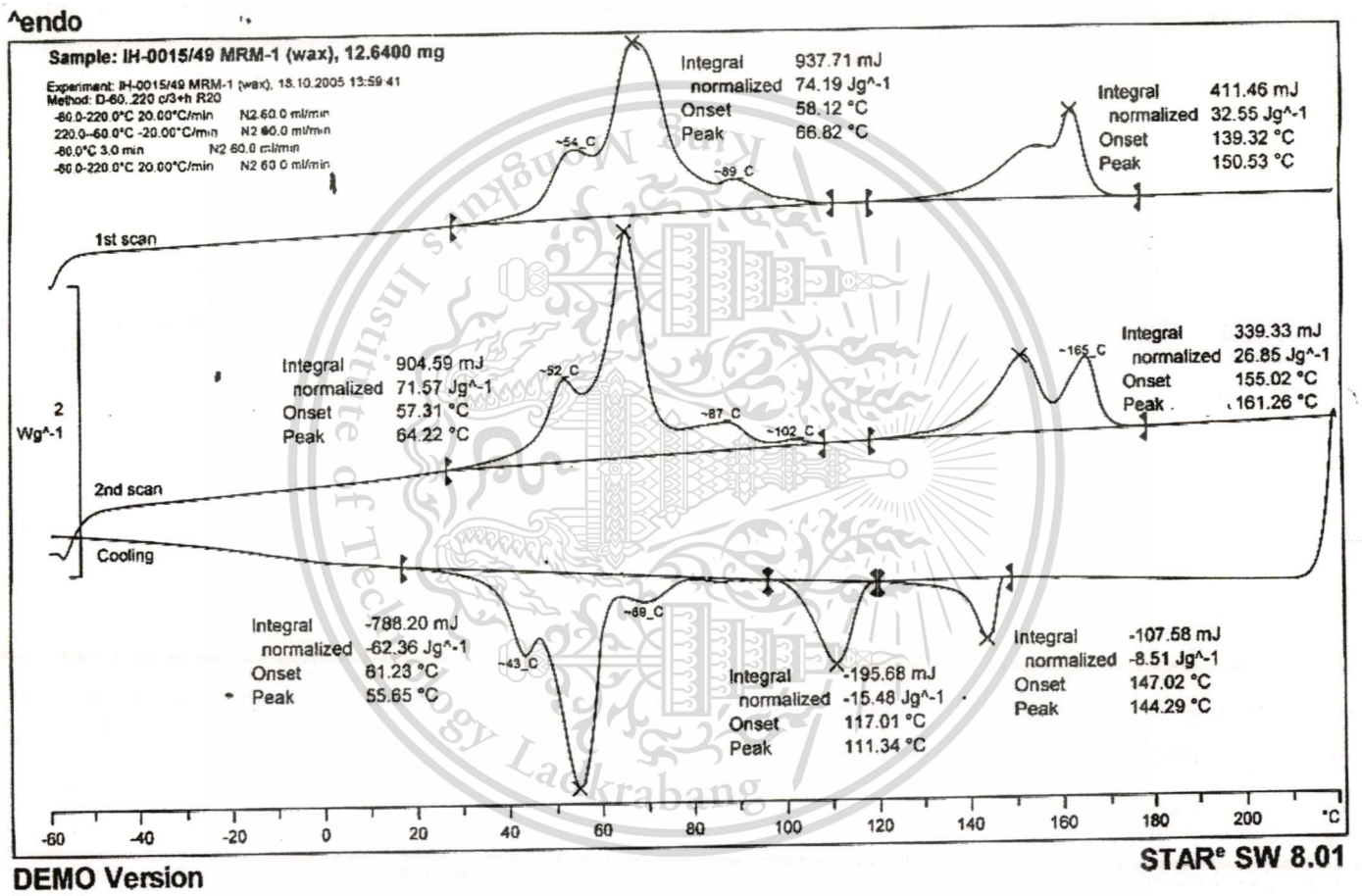

Figure B-5 Scanned image of DSC of commercial binder (MRM) under nitrogen atmosphere

Appendix B-6: TGA results of polypropylene 3342 M

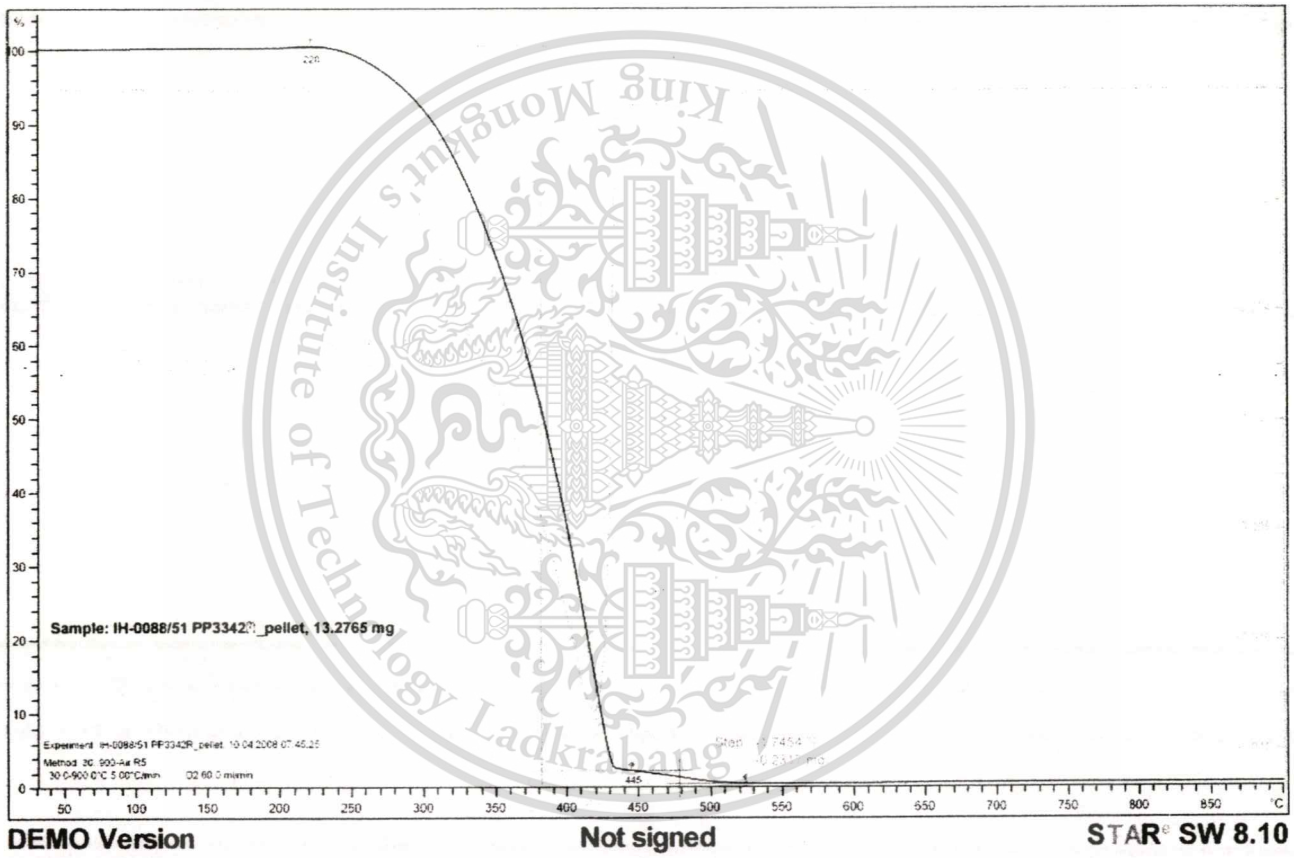

Figure B-7 Scanned image of TGA of polypropylene 3342 M under oxygen atmosphere

Appendix B-8: TGA results of paraffin wax

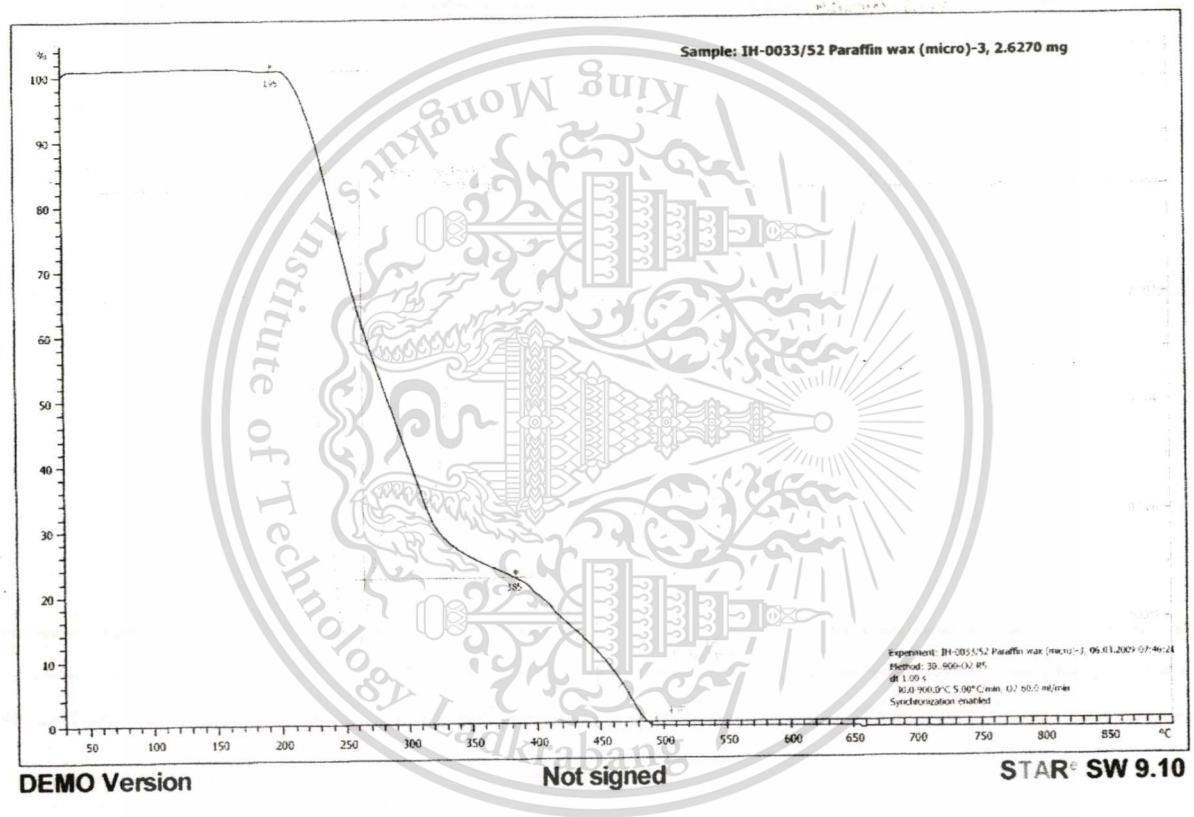

Figure B-8 Scanned image of TGA of paraffin under oxygen atmosphere

Appendix B-9: TGA results of stearic acid

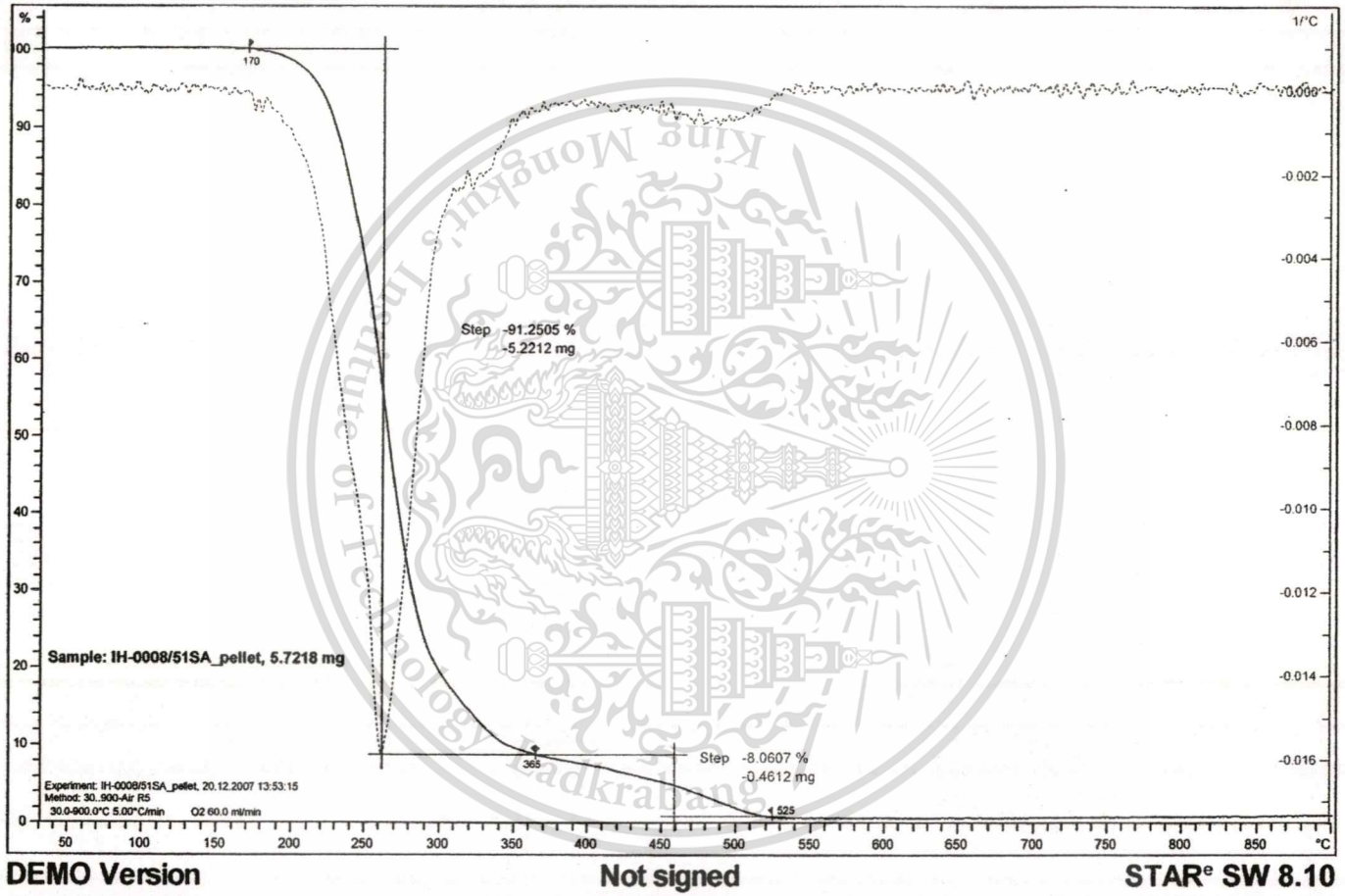

Figure B-9 Scanned image of TGA of stearic acid under oxygen atmosphere

Appendix B-10: TGA results of commercial binder (MRM)

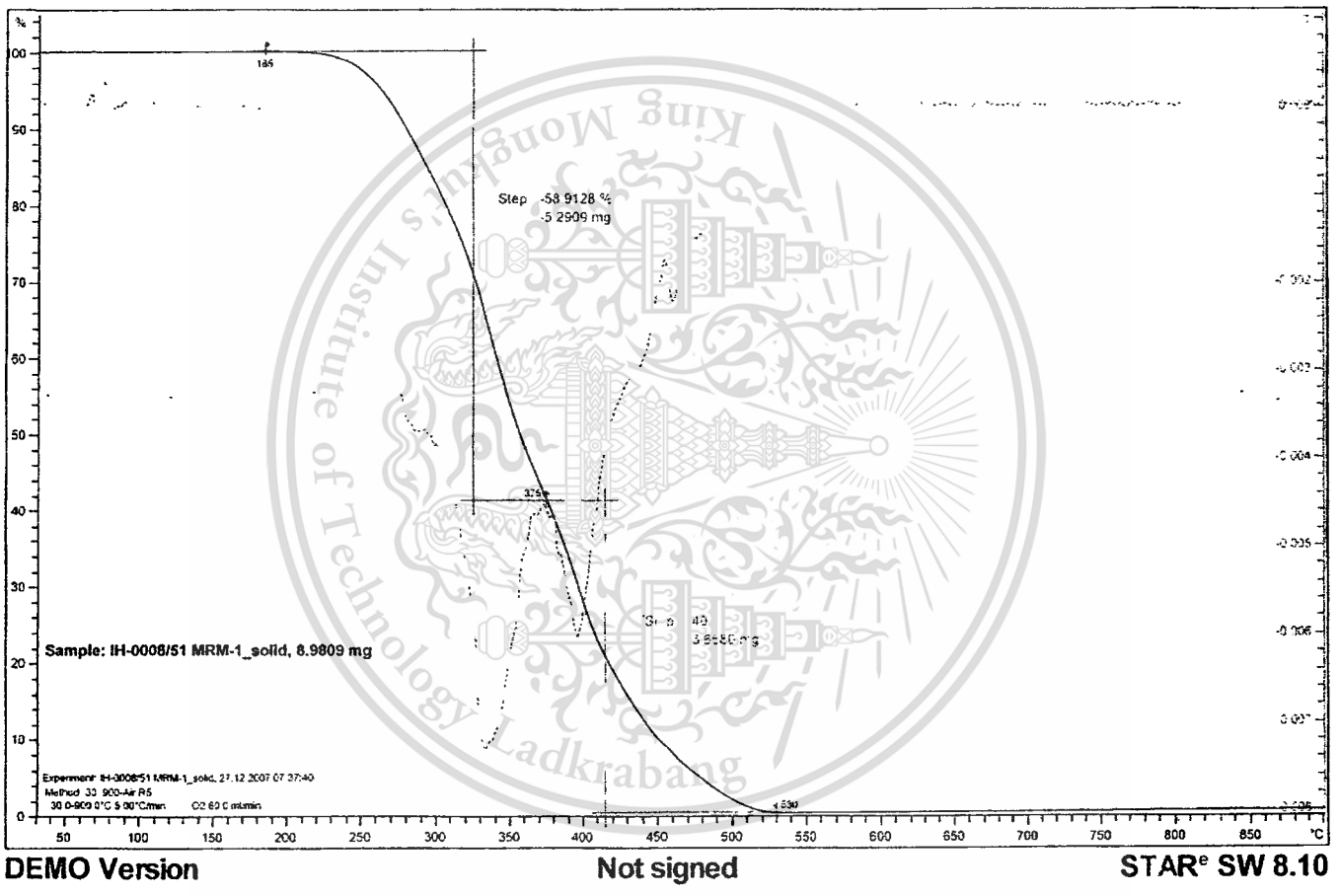

Figure B-10 Scanned image of TGA results of commercial binder (MRM) under oxygen atmosphere

Appendix B-11: DSC results of commercial binder (MRM)

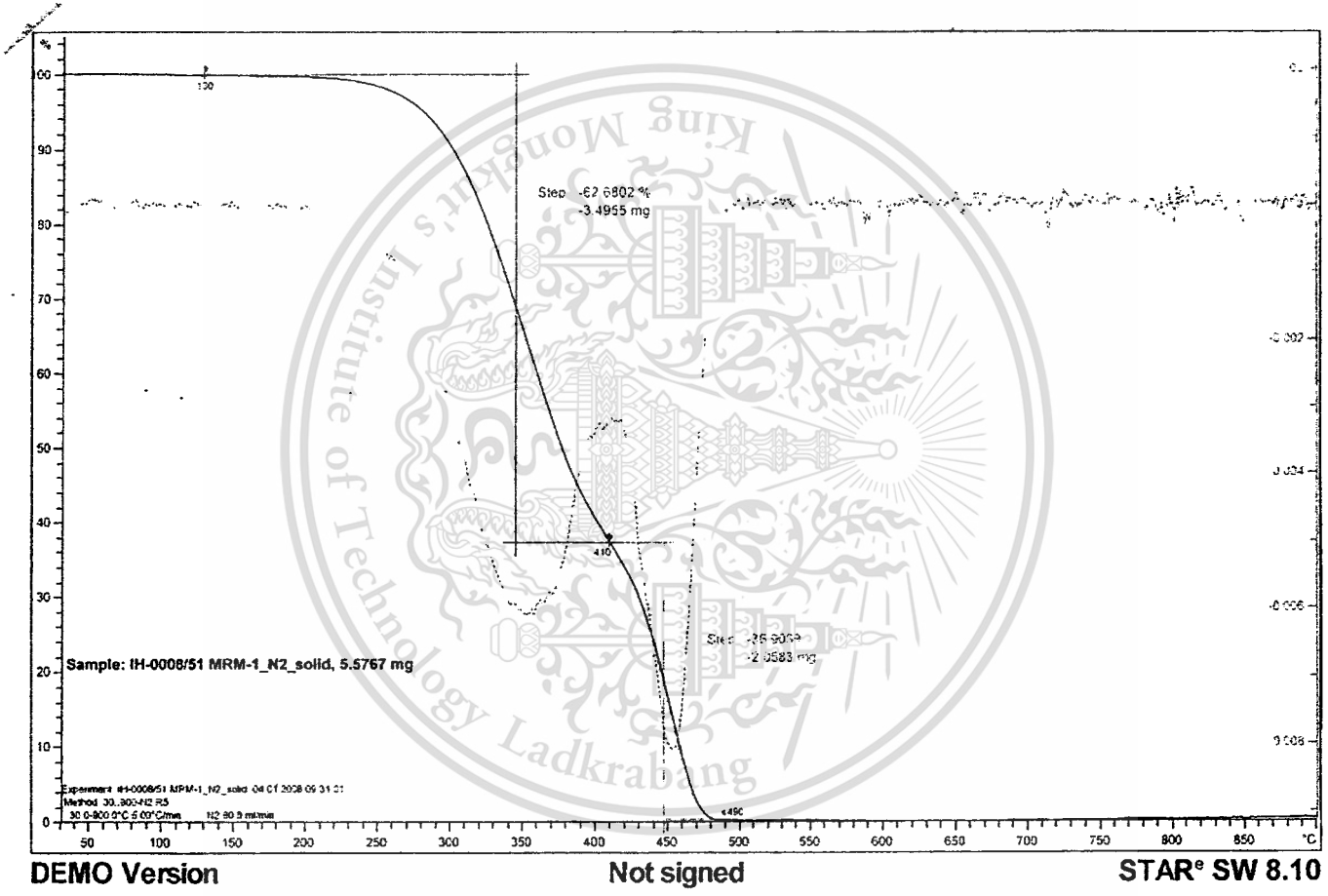

Figure B-11 Scanned image of TGA results of commercial binder under nitrogen atmosphere

APPENDIX C

XRD RESULTS AND INFORMATION

Appendix C-1: XRD result of pure Alumix 231 powder

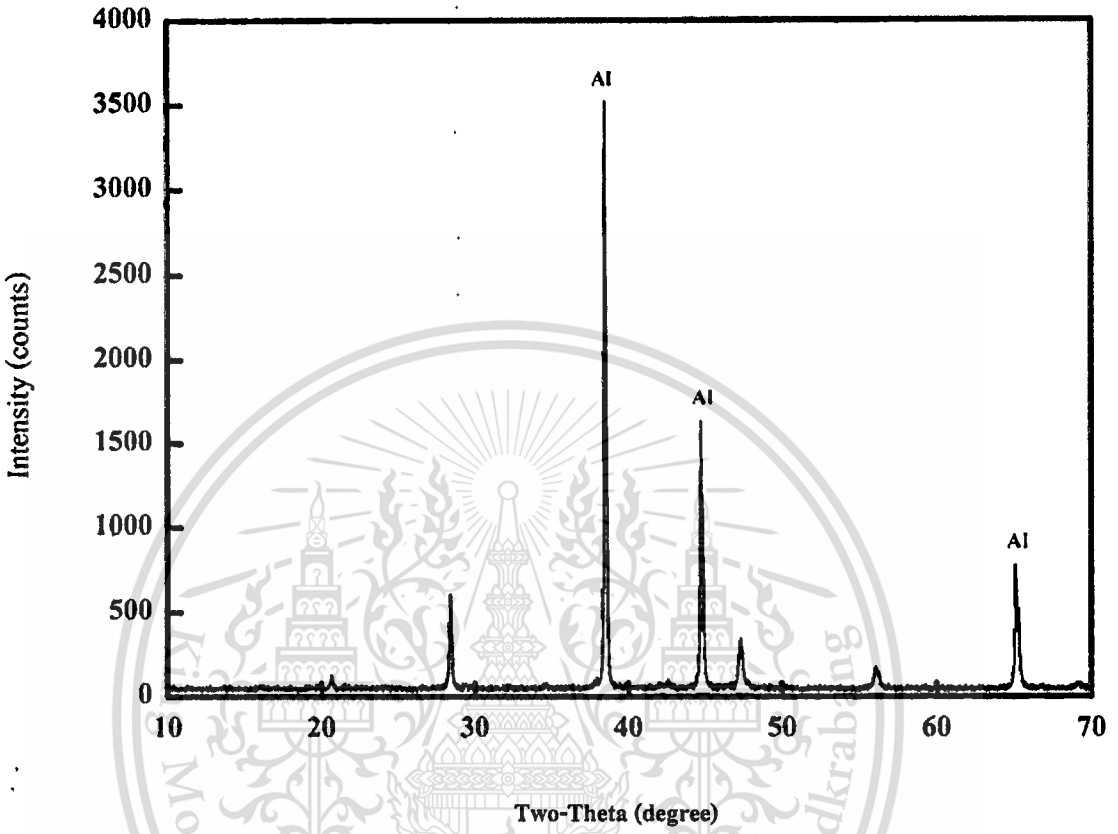

Figure C-1 XRD result of pure Alumix 231 powder

Appendix C-2: XRD result of MRM binder

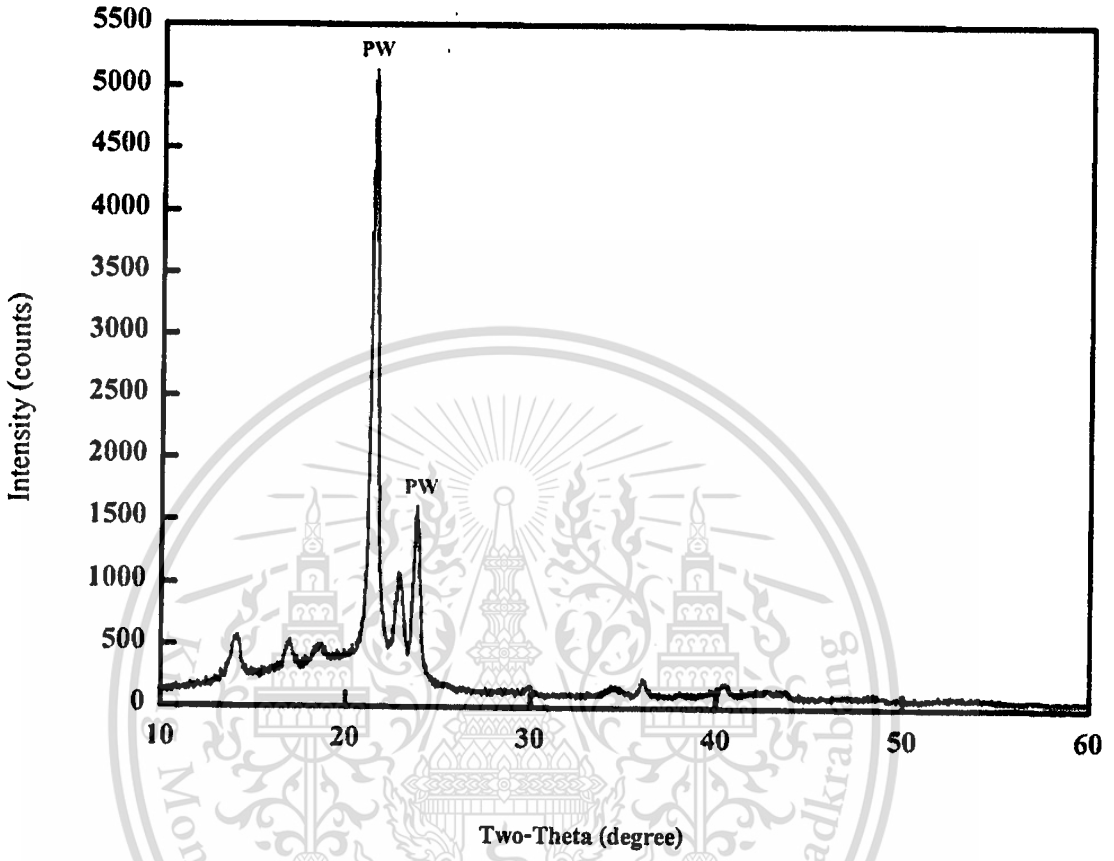

Figure C-2 XRD result of MRM binder

Appendix C-3: XRD result of feedstock from commercial binder

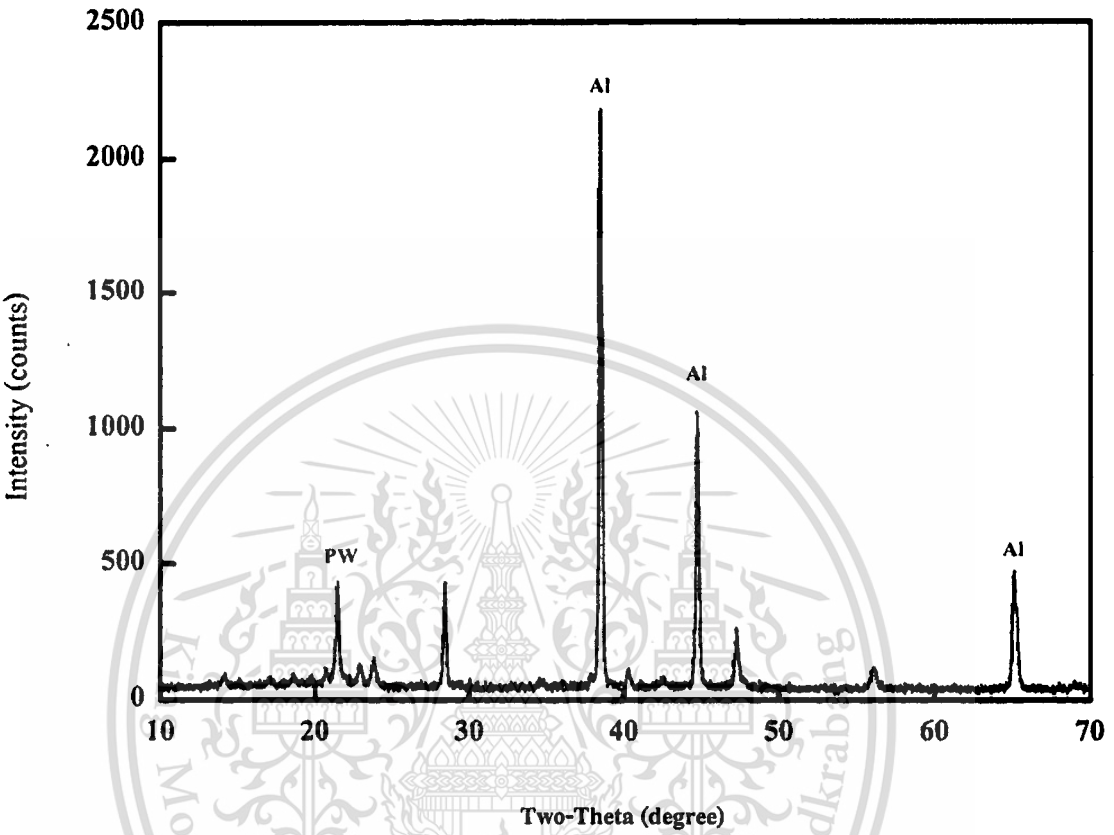

Figure C-3 XRD results feedstock commercial binder

Appendix C-4: XRD result of specimen with commercial binder after solvent debinding

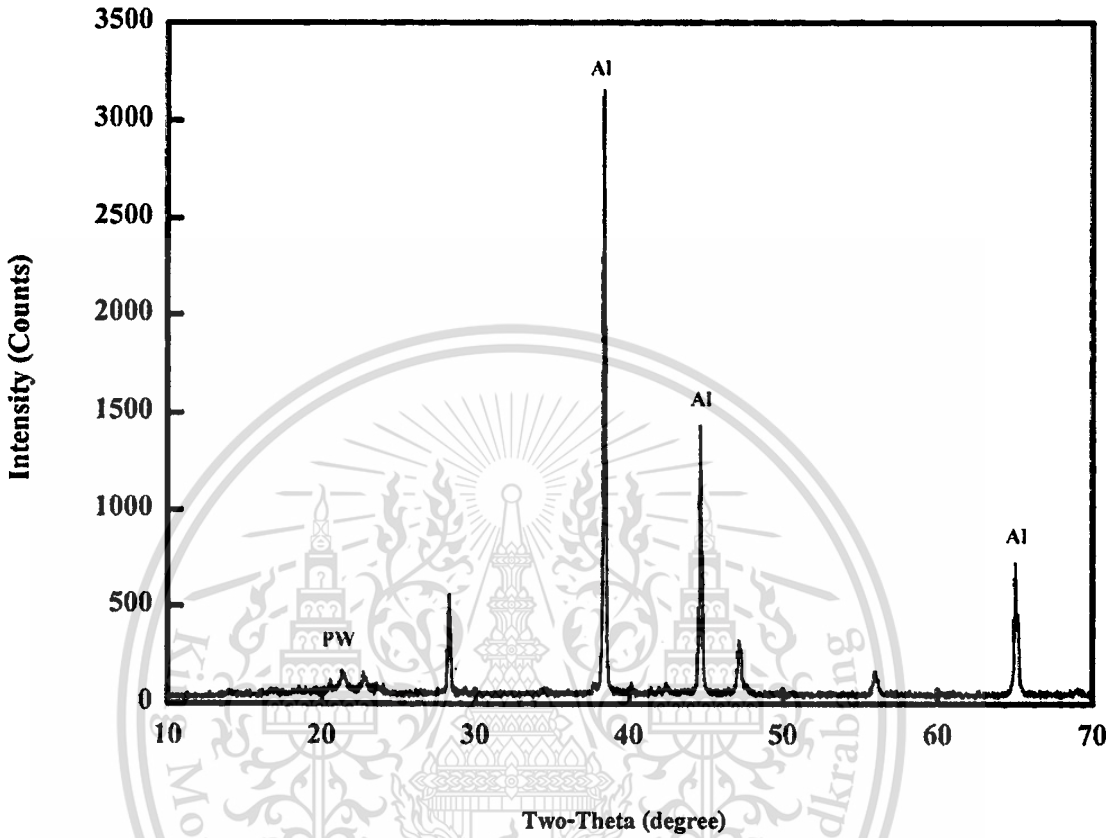

Figure C-4 XRD result of specimen after solvent debinded

Appendix C-5: XRD result of sintered specimen from commercial binder

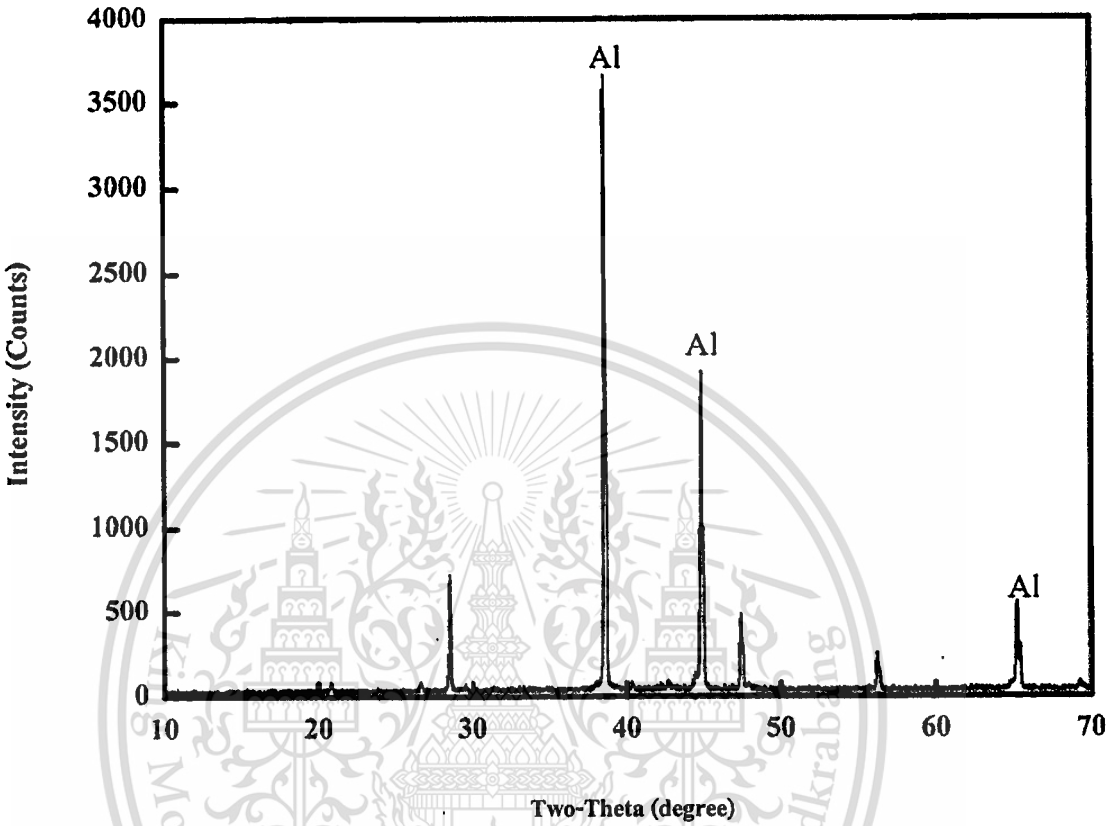

Figure C-5 XRD result of sintered specimen with commercial binder

BIOGRAPHY

Name: Mr. Tanapat Wongwattanakornchai

Date of Birth: July 30, 1985

Place of Birth: Bangkok, Thailand

Education:

2004-2008	B.Eng. in Mechanical Engineering, Department of Mechanical Engineering, Sirindhorn International Institute of Technology (SIIT), Thammasat University.
2008-2010	M.Eng. in Automotive Engineering (International program), International College, King Mongkut's Institute of Technology Ladkrabang (KMITL)

Honour and Scholarships:

2008-2010	Full scholarship for study in the master degree from National Science and Technology Development Agency (NSTDA)

Publications:

1. T. Wongwattanakornchai, A. Manonukul, P. Kansuwan, and K. Takahashi. "Effect of the Purity of Nitrogen and Present of Sacrificial Material on the Sinterability of Sintered Aluminium Alloy (Al-Si-Cu-Mg)". **International Conference on Materials Processing Technology**, Phuket, Thailand, June 2-3, 2011. pp 186-190.